LIGO

LIGO-E030392-00-D-

California Institute of Technology

July 2001 - December 2001

LIGO project :

Test masses suspensions modeling

Matthieu MUSSO

Mentors : Phil WILLEMS
Régis DUFOUR

SUMMARY

ABSTRACT

Detecting gravitational waves requires a huge precision when measuring free masses' displacements by laser interferometry. These masses, symbolized by mirrors, are suspended by fibers on both sides in order to move freely. The suspensions are really important considering noises disturbing the measurements, especially the thermal noise. In this report, are modeled and analyzed four different designs of mirrors' suspensions. The main goal of this modeling is to reduce, as far as possible, the amount of stress at the interface between the suspension parts and the mirror. Two LIGO designs are compared to two other designs coming from the University of Glasgow in charge of the suspensions designs in Europe for the GEO project. The study seems to show that one of the LIGO's designs presents better results than other ones. This design has not to be considered as the final solution for LIGO II but the way to design and to model the suspension has to be enhanced. Another study, in the latest part of this paper, is about to prove that creep could be a serious deal for the suspensions. Here again, this second work is not finished yet.

INTRODUCTION

For a long time, scientists have been looking for the creation of universe through Astronomy. The only way to answer such a question is trying to get information directly from other planets of this universe. These data come to us as gravitational waves.

The idea of a Laser Interferometric Gravitational waves Observatory (LIGO) is to use the gravitational waves properties in order to inform us about phenomenon such as black holes, supernovae, planets collapses....

This project requires a precision of 10^{-21} to detect tiny displacements caused by gravitational waves. The interferometer measures the displacements of the free masses. The purpose of this study is to model the suspension of theses free masses, most sensible part of the interferometer. The most important part of the suspensions are fibers suspending each mirror as a free mass. The suspensions have to be designed so that they can deal with noises disturbing the measurements of the interferometer.

After presenting the principle of the interferometer, we will describe precisely the suspension general design and the goal of the study. Then, we will start to model the different parts of the suspension trying to figure out which one the four different designs is adapted to the problem. The last part of this report will deal with a study concerning viscoelasticity of materials used in LIGO.

1 L.I.G.O. (Laser Interferometer Gravitational waves Observatory) project presentation [1]:

1.1 Generalities about gravitational waves:

Gravitational waves are ripples in the fabric of space and time; they move as oscillations of gravitational field. They are produced by violent events in the distant universe. For example, they can be produced by the collision of two black holes or by the cores of supernova explosions. Accelerating masses, as accelerating charges produce electromagnetic waves, emit gravitational waves, they travel to Earth bringing information with them about their origin and about the nature of gravity.

The polarizations are made along orthogonal directions like an "+" (fig.1) or like an "x" (fig.2):

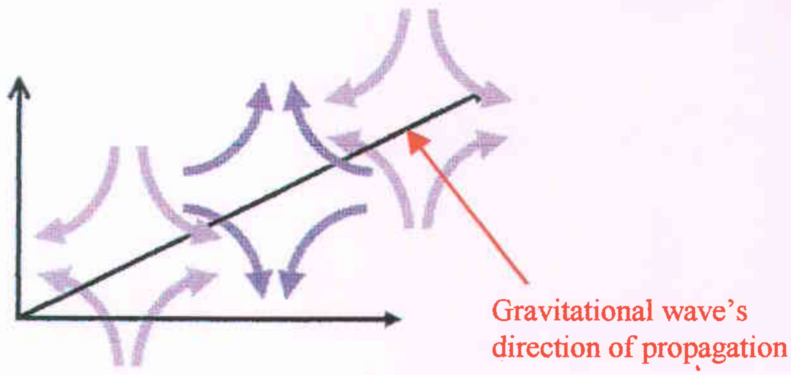

Fig.1-" + polarization"

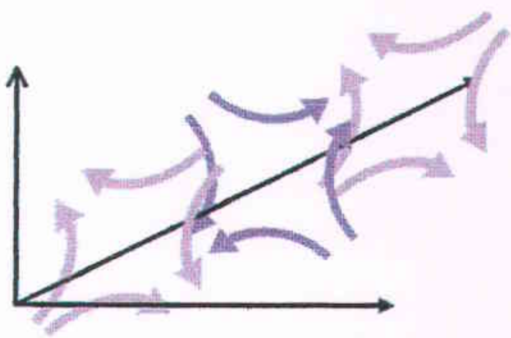

Fig.2 – "x polarization"

A small mass placed at several points along the wave shown above will be stretched along one axis and squeezed along the perpendicular axis, then one-half cycle later, the phenomenon reverses.

1.2 LIGO project description:

1.2.1 Scientific goals:

The principal goal of this project is to detect and study astrophysical gravitational waves and use data from them to do research in physics and astronomy. Hence, LIGO will support studies concerning the nature of gravity, the structures of black holes, and the equation of state of nuclear matter. It will also measure masses, collisions and distributions of black holes in the universe.

The technology for LIGO has been developed for 30 years. When it reaches maturity, this observatory will be open for use by the national community and will become part of a planned worldwide network of gravitational wave observatories.

1.2.2 General principle:

The very general principle is to measure the effect of gravitational waves on masses in the two perpendicular directions of the polarization as we saw before. Thus, the construction of a L-shaped antenna approximately aligned with the polarization of the wave can be a solution to detect the squeezing of space along one arm of the antenna and the simultaneous stretching of space along the other arm, as shown below:

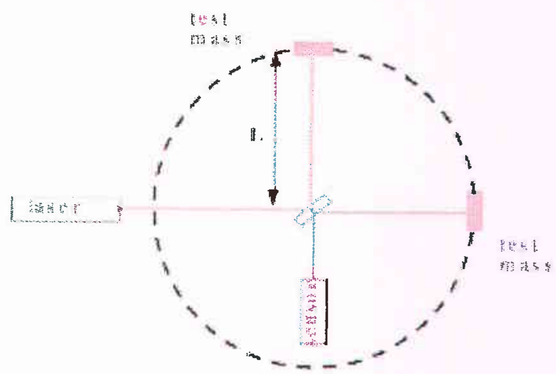

Laser light, because of its well-known wavelength, is here used to measure the squeezing and stretching of space (L variations). These squeezing and stretching is very tiny: for example, the amount of squeezing and stretching of space that is predicted to occur such as the coalescence of a pair of neutron stars 100 million light years from Earth is about one part in 10^{22}. Basically, what is really measured is the "strain" of spacetime, the fractional amount of squeeze or stretch in the length of each arm. This means that the effect measured is greater the longer the arm becomes. That's why each arm's length is equal to 4 km to get a precision of 10^{-21} during the measurements. One can consider the following drawing to explain the mechanism of the interferometer:

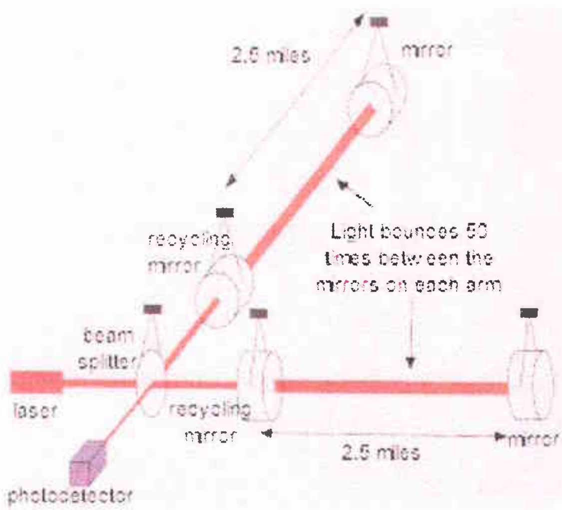

The "Fabry-Perot" mirrors (recycling mirrors on the drawing) are considered here as test masses. Since wires suspend them, one can assume that they also are free masses from a mechanical point of view.

The beams reflect laser light off mirrors at either end of the L and then are recombined at the vertex of the L. The squeezing and stretching of space produced by gravitational waves causes differences in the arrival times of the light from each arm. Light that propagates down the arm, which is squeezed, arrives back at the vertex of the L a little ahead of the light, which went down the arm that was stretched. The gravitational wave is detected as a variation in the phase of the light at a photodetector placed near the vertex of the L.

In order to increase the sensitivity of the interferometer, light coming from the laser bounces back and forth between the input and end of the mirrors in each arm about 50 times before re-emerging and being compared to light that did the same thing in the other arm.

1.2.3 Noise:

The effects of gravitational radiation are very tiny and they must be distinguished from background noise sources. A noise-induced fluctuation of one end mirror towards the vertex and the other end mirror away would mimic the effect of a gravitational wave. The major noise sources that causes this to happen are:

- Seismic noise coming from ground vibration (stretches and squeezes the arms of the interferometer),

- Thermal noise resulting from heat energy and causing vibrations,
- Shot noise such as statistic noise limiting high frequency response,
- Electronic noise in the control and acquisition data systems,
- Laser stability in frequency and intensity.

In order to moderate the seismic noise, which is the principal cause of test mass motion, a Seismic Attenuation System (SAS) is designed allowing low frequency seismic attenuation and high stability. One the one hand, the SAS provides seismic isolation sufficient to drive the seismic noise of the detectors well below the thermal noise. On the other hand, it suppresses the residual rms. motion of the test masses for easy locking and reliable/stable operation of the detectors. To do so, the SAS is made as an assembly of cascaded low frequency mechanical attenuators plus an inertial damping control system such as this one: [2]

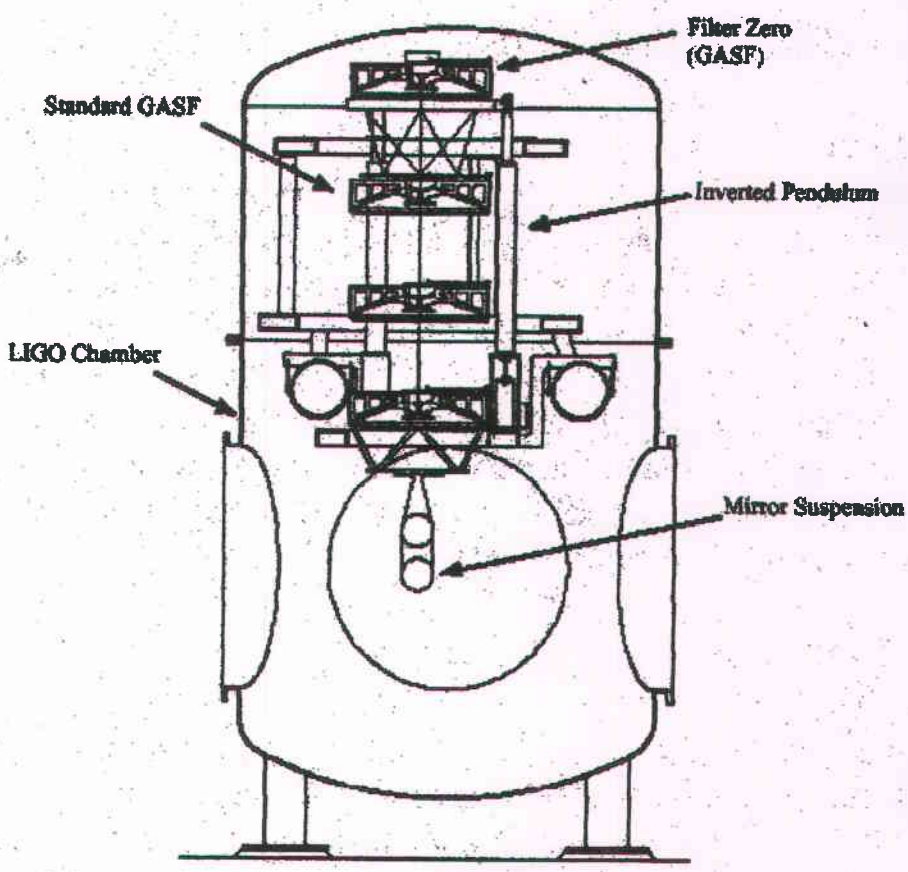

Fig. 1. SAS configuration for LIGO II

An inverted pendulum (IP) for horizontal isolation is fixed on a structure that is supported by tubes connected to the ground via piers. The IP hosts an ultra low frequency Geometric Anti-Spring Filter (GASF), which is called filter zero for vertical isolation. The IP and the filter zero form a pre-isolator stage. Three GASF are attached on the filter zero for the isolation in all degrees of freedom. A test mass is supported by suspension system below the last GASF.

2 The test masses suspensions:

2.1 Presentation [3]:

As shown on the figure above, the test masses (mirrors) are suspended to the last GASF. Usually, these masses are part of triple or quadruple pendulum based on the design of the GEO 600 project (equivalent project between Glasgow and Hanover in Europe). One Advanced LIGO suspension uses a triple pendulum composed of the upper mass (situated under the last GASF), the intermediate mass and the test mass such as described below (schematic of a triple pendulum based on the GEO design):

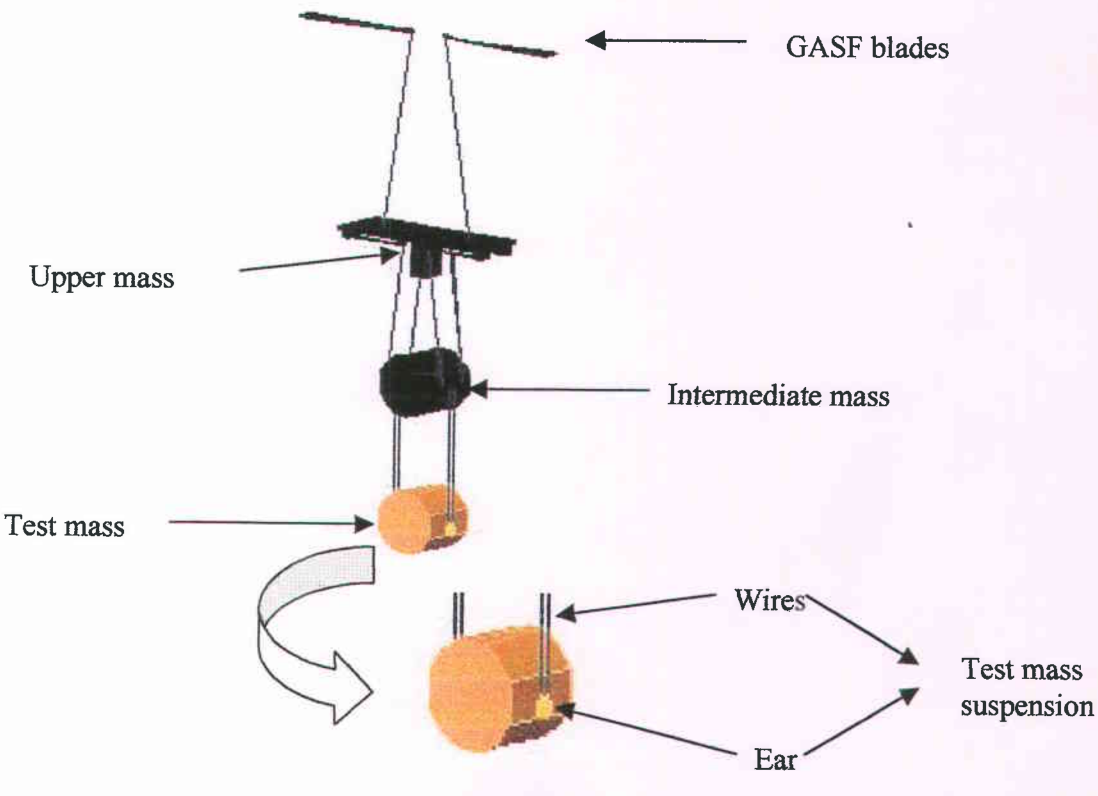

As one can see, on both sides, the test mass is suspended to the intermediate mass by two wires welded to an "ear" which is itself bonded to the mirror. The three masses have about the same weight, and the intermediate one has exactly the same dimensions as the test mass so that the wires can remain vertical.

2.2 Thermal noise and quality factor (Q) :

At the last stage of the pendulum, there are two major types of thermal noise: the pendulum thermal noise and the mirror thermal noise. Pendulum thermal noise results from the free oscillations of the test mass, the noise intensity is proportional to the velocity of the test mass. Mirror thermal noise is caused by the deformations inside the mirror according to its modes.

In order to reduce both thermal noises in the pendulum, materials must be chosen with a high quality factor (Q). For a harmonic oscillator, the Q factor of a material can be defined as $Q = f_0/\Delta f$, where f_0 is the resonance frequency of the oscillator and Δf is the bandwidth (taken at half maximum power) at f_0. Then, since thermal noise is inversely proportional to Q (except at $f = f_0$); the more Q, the less thermal noise we have.

Increasing Q will result in decreasing thermal noise above and below f_0. On the contrary, increasing Q will increase thermal noise at f_0; that's why pendulum's resonance has to be avoided.

2.3 Material, geometry, bonding and welding:

The material chosen for the test masses, the ears and the wires is fused silica (SiO_2 glass), which means that the bottom stage of the pendulum is monolithic. Tests are being made to use sapphire for the mirrors but we better use fused silica for modeling at this time. Since thermal noise mostly comes from this part of the pendulum, fused silica has been chosen for its high Q factor. Actually, Q varies with mirror and fibers (wires) fabrications but also with bonding and welding quality.

To bond correctly the ears to the mirror, both surfaces of the ear and the mirror have to be polished such as their roughness criteria does not exceed $\lambda/10$ where $\lambda = 632.8$ nm. Then, a small drop of a strong base solution (pH $\approx$ 13) is placed between both parts of glass and, by waiting several days the bond is formed. This solution is made of KOH or $NaOH+SiO_2$, which create links between both surfaces by precipitating after the water of the solution evaporates. The volume of solution used is very small; it's 1 $\mu L/cm^2$ to 10 $\mu L/cm^2$ for both of them. Of course, since both surfaces have to be plane, the mirror is machined on each side. If we look carefully at the picture in 3.3.1, we can see that the bond is not correctly formed. There are actually a few bubbles confirming that the solution is not equally distributed. These bubbles are very dangerous for the bond since they act as stress focus points and later, as cracks. Here is the importance of the bonding.

Concerning the welding, the fiber and the "legs" of the ear are put together in contact and warmed up (oxygen/hydrogen gas) until they melt and fuse correctly (see picture 1 in annex).

Assuming that these operations were correctly done, we can give the following results when measuring Q for the mirror and fibers (homemade measures):

- $Q_{mirror} = 1.8\times10^7$

• $Q_{fibers} = 5\times10^8$

Both these Q factors are considered as very good for this project even if they limit a little the sensitivity of the interferometer.

Sapphire was the first choice for LIGO II as it would be more appropriate to this problem than fused silica (with sapphire, $Q_{mirror} = 2\times10^8$). But as there are technical barriers and unknowns in sapphire development, fused silica is used for the current research. The mechanical and physical properties of fused silica are given in annex. The length of the fibers between the test mass and the intermediate mass is 600 mm and they have a 0.75 mm diameter (circular section). The test masses for the advanced LIGO project have cylinder geometry, as they are mirrors, with a 31.4 cm diameter and a 13 cm thickness. Once these test masses are polished, they can behave as "Fabry-Perot" mirrors such as the ones shown below:

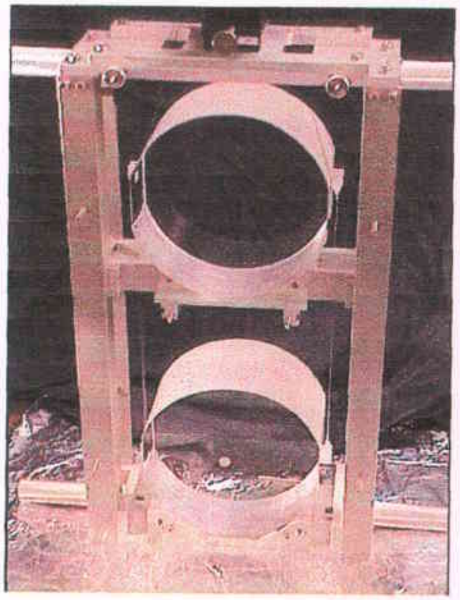

2.4 Modeling purpose:

This work principally deals with the test mass suspension. Actually, it consists in finding new ears design in order to reduce the amount of stress at the interface ear/mirror. Hence, after designing the ear, my interest will be in modeling the whole test mass suspension to compute the stress distribution in the bond using a finite element analysis (FEA).

• Design:

As we will see in the next part of this report, the ears, the fibers and the mirror are designed and assembled by using a CAD software: "AutoCAD".

To introduce the goal of this design, let's consider a very simple drawing of the suspension:

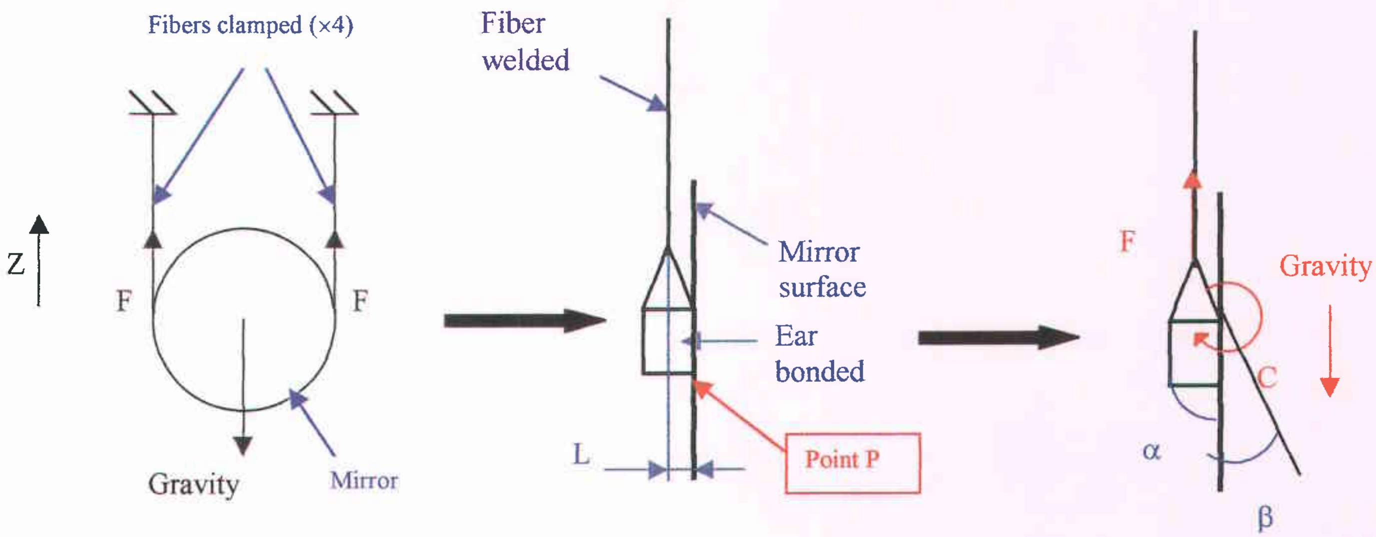

Assuming that the main efforts in the suspension are vertical along the x-axis, we can expect shear stress as the most important stress in the bond.

However, if we consider only one side of the mirror, in response to the action of the gravity on the free mass, there will be reaction forces F as shown above. Since there is a little distance L between the fiber and the mirror surface, it will introduce torques such as C trying to pull the ear away from the mirror: this is one of the most important causes of stress at the bottom of the bond layer (point P). That's why the new designs will be made in order to reduce as far as possible L. Moreover, reducing L will allow us to get closer from pure shear, which is well known to be strong compared to tension normal to the bond..

If we keep in mind the risk of cracks formation described in 2.3, we also have to consider the tension perpendicular to the Z-axis in the plane of the bond. Whereas compression is not dangerous, the tension stress in this direction could make the growing of these cracks easier. Then, resuming, we will have to compute three types of stresses: the tension perpendicular to the vertical axis in the bond, the stress normal to the bond caused by the torques and the shear stress in the bond.

A good way to represent the shear is to compute the maximum shear stress distribution using the Tresca stress defined by $\tau_{max} = 0.5*\text{MAX}(\text{abs}(\sigma_1-\sigma_2), \text{abs}(\sigma_2 - \sigma_3), \text{abs}(\sigma_3 - \sigma_1))$; where σ_1, σ_2 and σ_3 are the stresses in the principal directions. Then, we will compare the maximum value to the breaking stress of the bond, which was measured at 20 MPa.

- FEA:

Each complete suspension model (mirror + ears + fibers) will have to be analyzed using a finite element code. To do so, we will principally use the "Mechanical desktop " software package. Since this software contains "AutoCAD" and the finite elements code "Algor", importing drawings to the finite elements code won't cause any problem. This analysis will allow the computation of the stress distribution in the bond in each direction of the space. It will also give us an idea of the deformed shape of the entire test mass suspension. Before each analysis, the conditions of calculations will be justified (finite element choice, assumptions, load, boundary condition, …).

A 2-D modeling will be presented as an introduction, trying to figure out the different assumptions and simplifications we can make about this modeling. Starting from this, the 3-D modeling will be performed in this order:

- We will first study two designs coming from the university of Glasgow (Scotland) by drawing them, computing the stress distribution at the bond and testing them when doing experiments,
- Hence, we will be able to compare experimental and computed stress distributions,
- The same kind of work will be done for two other "homemade" designs, except the experiments, as we were late on the schedule,
- Hence, by comparing the four models results, one particular design will be advanced as a **possible** solution for LIGO II.
- At last, in the fourth part of this report, another type of analysis will occur. It will deal with the thermoelastic study of a fused silica/sapphire bond.

3 Bonds modeling:

3.1 2-D studies:

By designing a 2-D model of one of the first suspensions LIGO worked on, we will be able to notice the different stress focus points around the ear section and we will also learn about the stress distribution in the bond. This will be useful when starting 3-D modeling.

3.1.1 Suspension design:

The first suspension for LIGO II used four ears, two on each side of the mirror, connecting four fibers such as the following one coming from the GEO design:

The ear is designed as a simple prism, which can be easily drawn using the "Ansys" code:

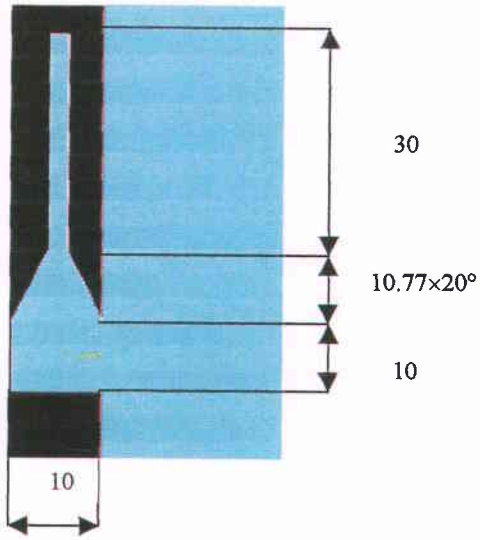

By comparing this drawing to the picture above, we can notice certain differences concerning the fiber. First, its diameter on the picture varies due to the welding, passing from 2-3 mm to <1mm (after the welded part) in order to increase its Q factor. As we won't study the fiber itself but the connection between the ear and the mirror, keeping a constant diameter (2 mm) superior to the real one is not a big deal. Dimensions inferior to 1 mm could cause troubles in the meshing. Also, the length of this fiber (30mm) is really inferior to the regular one (600mm). Here again, this won't cause any trouble in the modeling since the effort applied on the ear by the fiber is not proportional to the length of the fiber.

3.1.2 FEA:

Starting from this design, several analyses were made especially trying to model the bond layer between the ear and the mirror.

First of all, we can try to simplify the model by considering its vertical symmetry: the load (gravity applied at the center of the test mass), the boundary conditions (each fiber clamped on top) and the geometry are symmetric along a vertical axis passing through the middle of the suspension. Then, we can consider only half of the design, which can reduce the time of calculation.

Each 2-D model will have the same load, boundary conditions as the following ones (horizontal view):

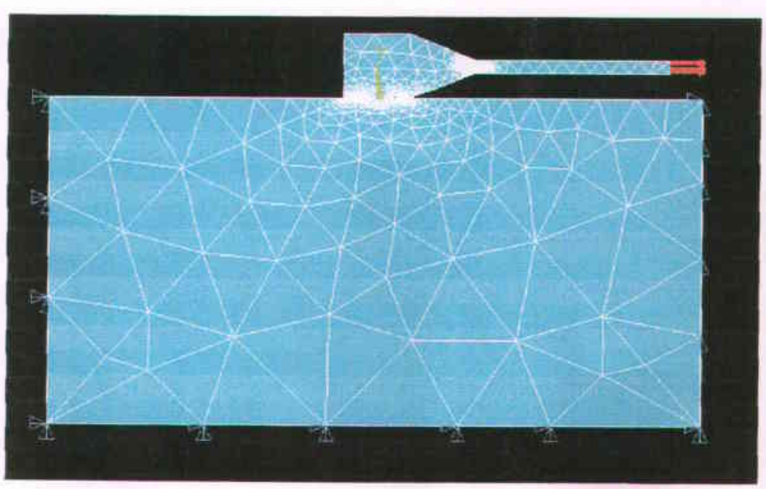

The mirror and the ear are both in fused silica.

We consider the mirror as a semi-infinite mass, that's why we clamp it. The load (in red) is applied on the top line of the fiber; this is a tension effort equal to the quarter of the mirror weight:

$$P = \frac{W_{mirror}}{L} = \frac{Mass \times gravity}{\Phi_{fiber}} = \frac{V_{mirror} \times \rho_{SiO_2} \times gravity}{\Phi_{fiber}} = \frac{0.001 \times 2210 \times 10}{0.002} = 11124\, N/m$$

Hence, in 2-D modeling, the effort F is F = P/4 = 2781 N/m for one fiber.

The model is meshed with a planar triangular element called PLANE2. This element has 6 nodes (3 nodes at each corner and 3 mid-nodes), it's well adapted to irregular mesh and it has quadratic displacement behavior. The triangular shape allows refining the mesh pretty well at the interface, especially at each extremity point of the bond, and also at the limit between the ear and the fiber. The bond interface is here considered as line shared by the ear and the side of the mirror. After a short time of computation, we get the following stress distribution for σ_{xx}:

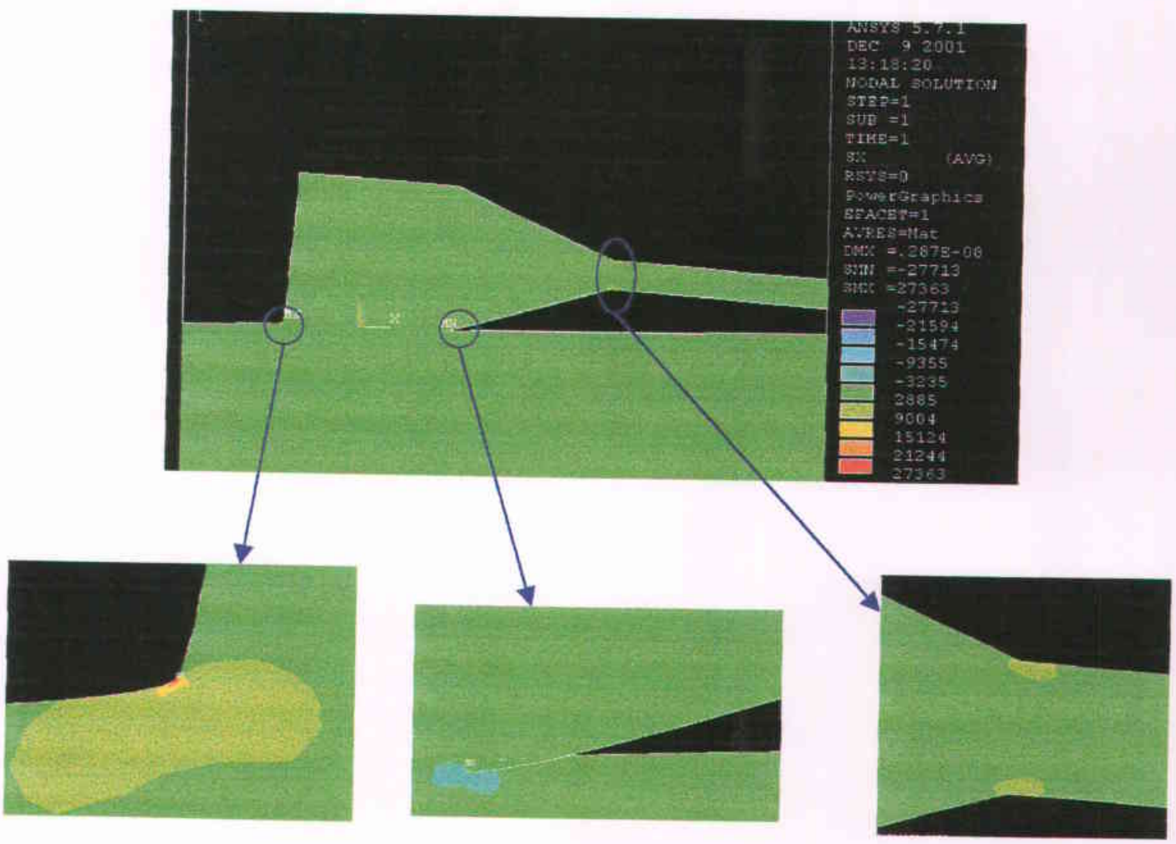

The σ_{xx} distribution (x along the bond) is uniform in the suspension. Regardless to the bond, we have two sensible points at the extremities of the interface. A maximum stress is located at the left extremity (point P, cf. 2.4) and a minimum at the right extremity. The minimum has actually the same intensity that the maximum one but is acting on the opposite way creating compression. Actually, what happens is that the mirror is pushing the ear on the top and pulling it on the bottom in response to the torques C described in 2.4. The deformed shape is a good proof of the mirror's; the stress distribution along the bond in the y direction varies from compression (top) to tension (bottom) as shown on figure 1 (in annex) for Syy. As a matter of fact, reducing this kind of stress will be the real priority of this study.

The stress focus found at the connection between the fiber and the ear reveals the importance of the welding especially if both shapes (ear "leg" and fiber sections) are not similar. If we consider now the deformed shape, we can notice that the fiber tends to be bended in the direction of the mirror; this effect is the result of the torques C (c.f. 2.4 again). Anyway, this effect is not really important compared to the stress in the bond.

Another study was made, trying to model the bond layer. To get a better model, we drew a layer (rectangle surface) between the ear and the mirror so that we could apply different material properties to it. Since the thickness of the bond layer was really small (100 nm, according to the measures), the stress distribution in the bond was not varying compared to the results above. Considering these results, we can assume that modeling the bond by a thin layer is not really important for our work.

Knowing now the principal criteria to respect, we can begin the 3-D modeling of the whole test mass suspension.

3.2 First bond model (Glasgow old design):

The university of Glasgow did an important work in the suspension design for the GEO project. This part will consist in modeling one of the two designs (the oldest one) they sent us so that we are able to compare them to our own designs.

3.2.1 Suspension design:

As explained before, we first have to draw the ear, the fiber, and the mirror to assemble them as the whole suspension. To realize the suspension, I use the "Mechanical Desktop" software. This software package contains AutoCAD as a design software and "Algor" as a FE software, hence, if we have complicated geometries, we'll be able to import directly the CAD file to "Algor", the IGES format is not needed.

- Ear design:

The ear is drawn using the 2-D plans sent by Glasgow (see Figure 2 in annex). Then, we obtain the following solid:

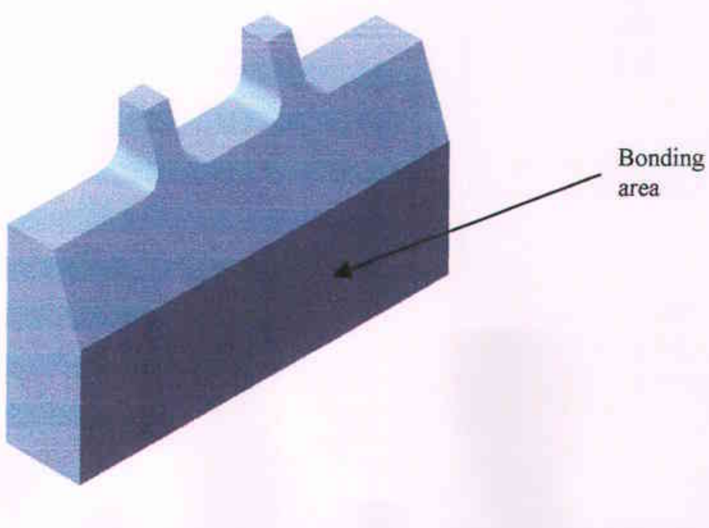

- Fiber design:

The fibers have a circular section (Φ=2mm), their regular length is 600mm but, since the load doesn't depend on this length, we will reduce it to 30mm to simplify the model.

- Mirror design:

The mirror dimensions are given in 2.3. Here's the drawing:

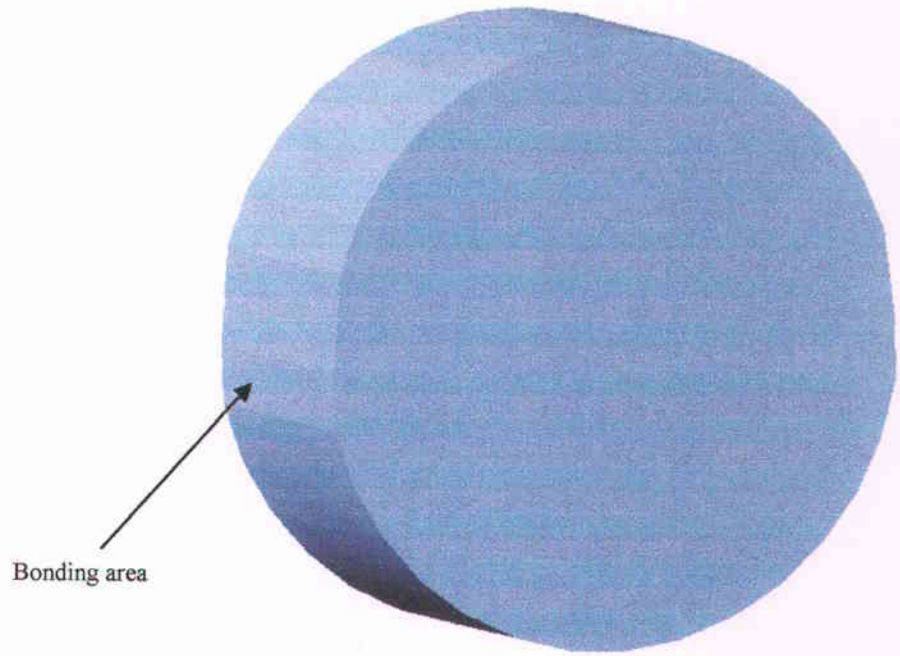

- Assembly:

Assembling the different parts above is really important regardless to the bonding of the ears. To model correctly the bond, we will apply constraints between the ears and the mirror by gluing together the surfaces of the ear and the mirror in contact. This operation is available with AutoCAD by creating several parts for the ears and the mirror and by assembling them with the "mate" command.

As we saw before for the 2-D model, modeling the bond layer will almost not change anything in the stress distribution since its thickness is very small.

As the legs of the ears have square sections, we will design the fibers as prisms (with a square section = $2\times2\ mm^2 \approx \pi\times1^2 = 3.14\ mm^2$), and a length of 30mm will be enough since this length does not act on the load intensity or distribution. Moreover, this simplification will avoid problems (due to complicated shapes) during the meshing; there will be continuity in the geometry. Anyway, during the FEA, we will focus on the stress distribution in the bond, which justify the geometry simplification for the fibers. Here's a 3-D wire frame of the model:

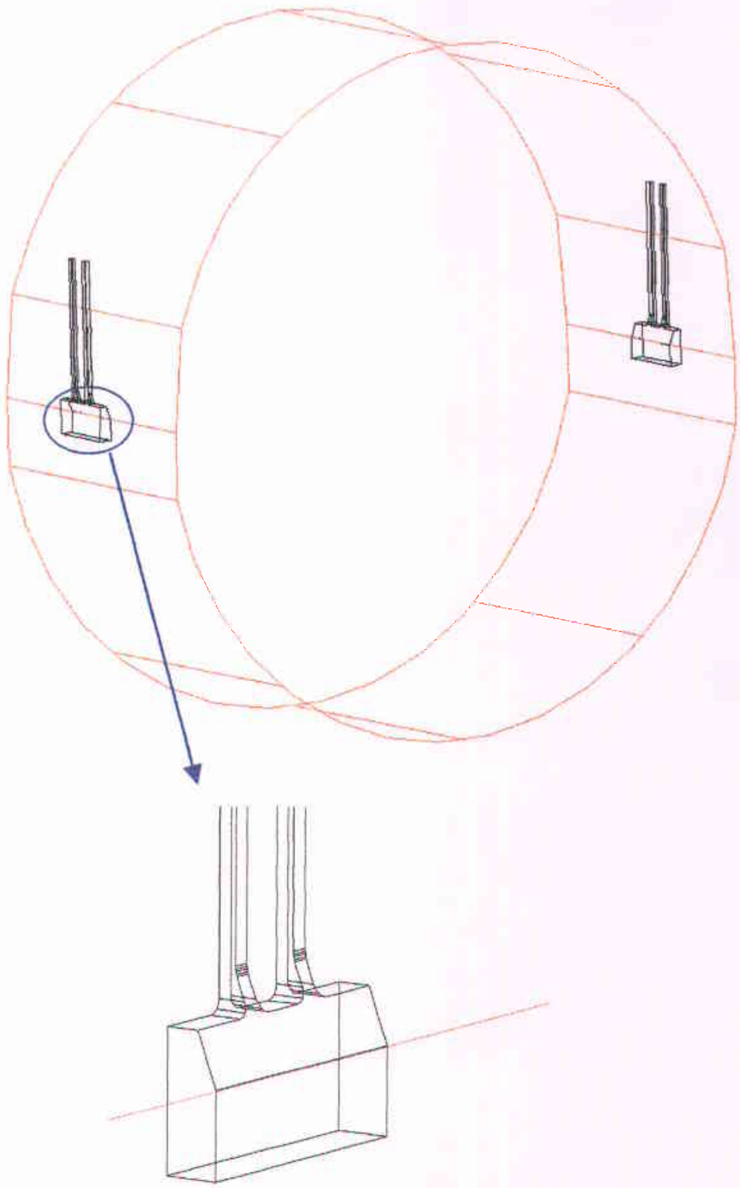

3.2.2 FEA:

To have a general view of the results, we will make the analysis for the whole suspension. In other words, we won't use the symmetry of the model here during the FEA.

We first tried to import the model to Ansys, which caused many troubles in keeping the AutoCAD geometry. So, we decided to use the FE code of Mechanical Desktop (Algor). Algor is built on two main parts: the CAD interface and the FEA editor. The CAD interface allows importing drawing files directly from the CAD software without converting the m into a specified format. This is really useful to conserve the geometry of the drawing. Once the model imported, you have to create a surface mesh first, and then, a solid mesh. The 2-D and 3-D elements library is less developed than the Ansys code and the mesh refining operation is more difficult to use. The meshing done, the model is transferred to the FEA editor where you can apply the material, the load, the boundary conditions, and choose the type of analysis.

Concerning the current model, we chose triangular elements as 2-D elements and tetrahedral elements as 3-D ones. It seemed to me that these elements would provide a good meshing refinement at the bond regardless to the geometry of the suspension. We can notice that since the geometry is really changing between the ear and the mirror and also since the mirror's dimensions are really superior to the ear's ones, the mesh is irregular at certain places.

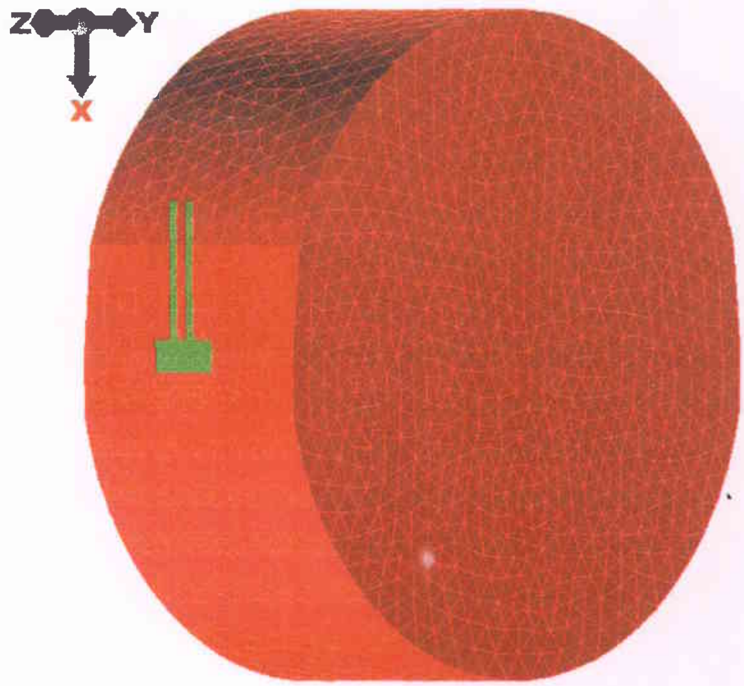

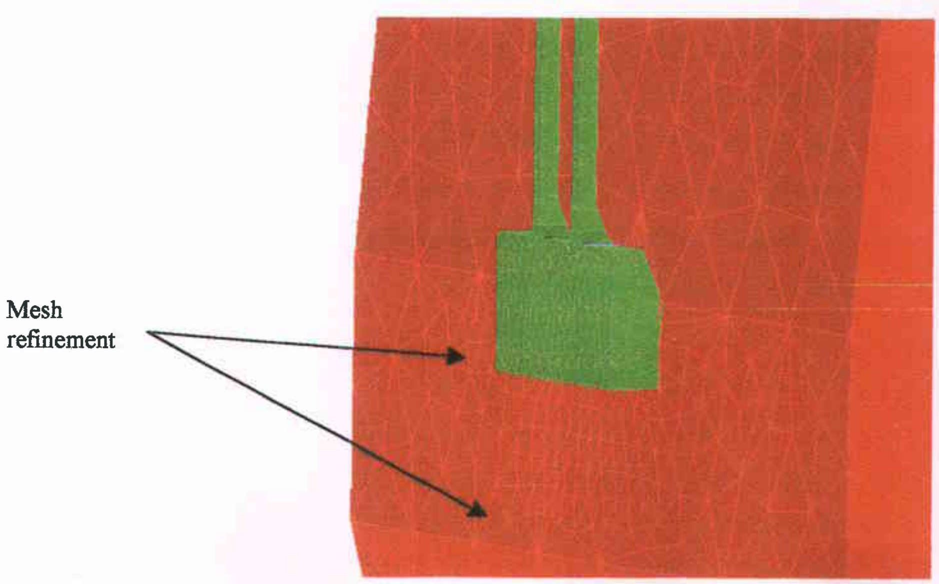

Using the FEA editor, we will perform a static analysis. The material specified is the same for all the different parts of the suspension: fused silica. The fibers are clamped on their top section and the gravity is applied at the center of gravity of the mirror. After performing the analysis, Algor gives the following shear distribution at the surface of the model:

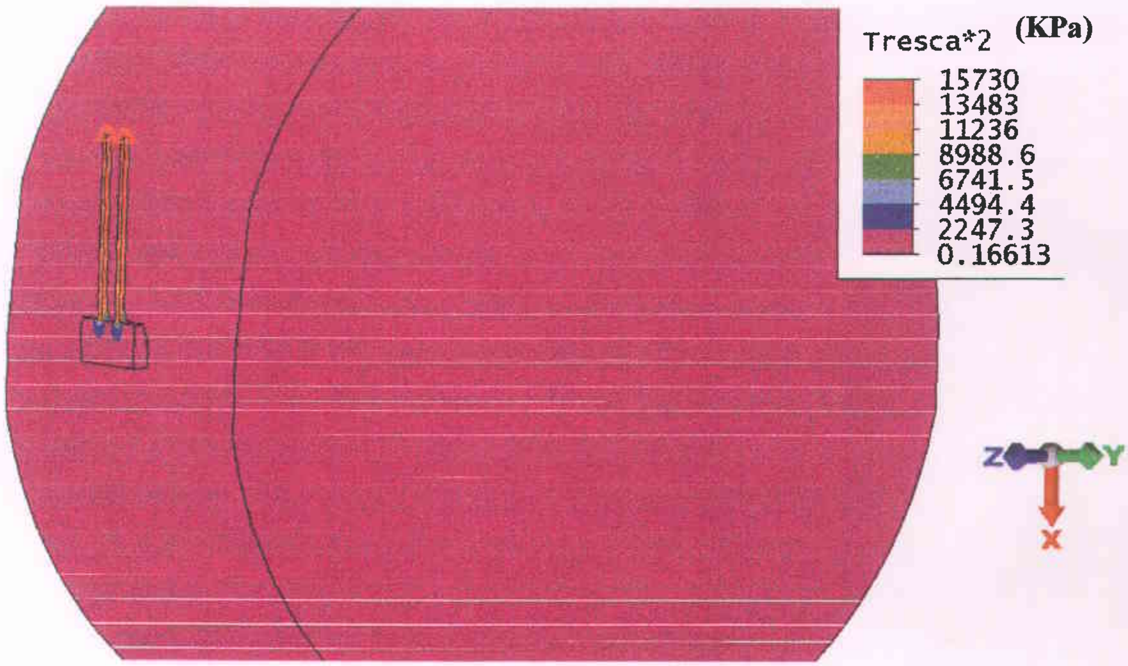

We have the same distribution on the other side according to the symmetry of the model.

Basically, Algor gives two times the Tresca stress as a result; the unity is the KPa (10^3Pa). The shear distribution is very low and constant at the mirror surface whereas it seems to vary a lot along the ear and also along the fiber. It seems that we get a maximum stress at the top of the fibers, which is not surprising since the fibers are clamped at this point. Displaying the stress distribution in the bond would be more interesting. To have an idea of the shear in the bond, we can display the surface of the ear in contact with the mirror by defining a cutting plane just between these two parts:

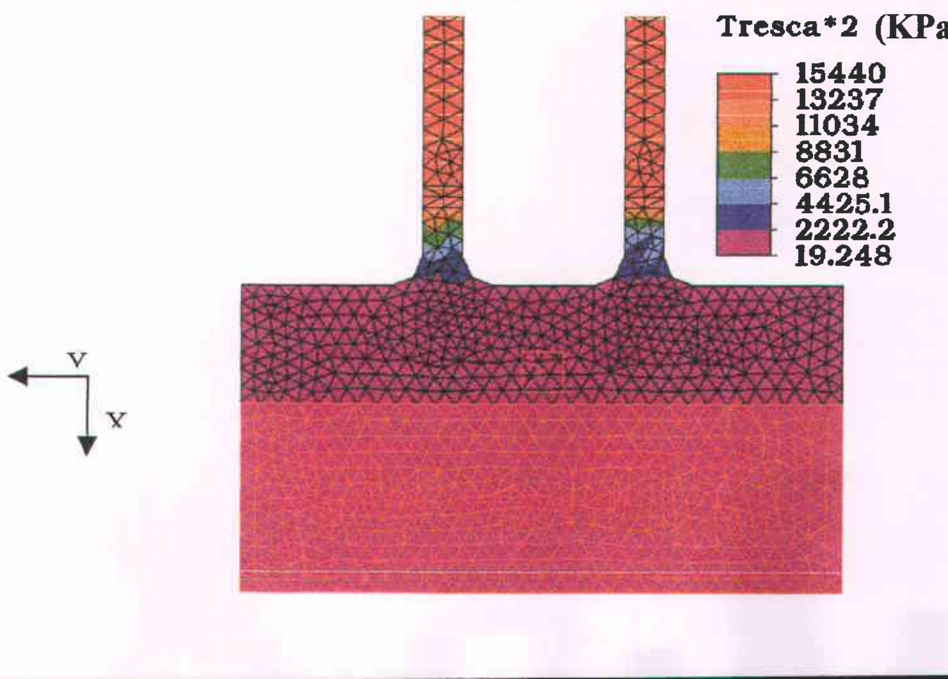

The shear distribution is constant in the bond. We can observe a variation of the stress along the fiber, especially after the welded part, the stress reaches its maximum value (7.72 MPa). The value of the shear in the bond is varying between 0.1 and 1.11 MPa, which are very small compared to the breaking stress of the bond (20 MPa).

Let's make another cut in the plan normal to the bond to display the stress caused by the torque C:

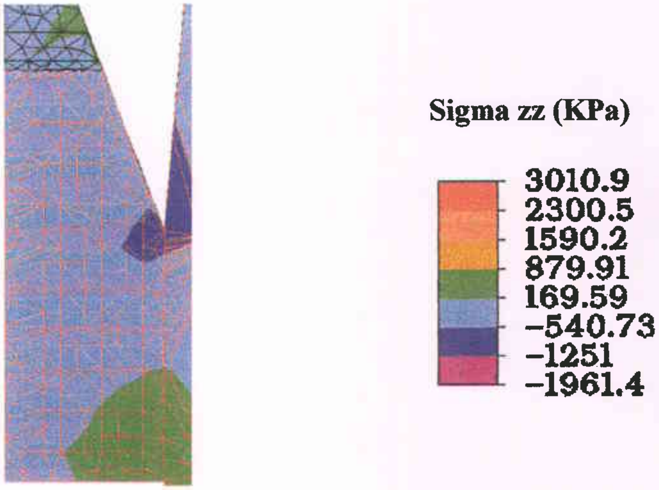

By referring to the color scale, we can easily see the effect of the mirror on the bond, pushing on the top and pulling at the bottom. The maximum compression stress applied by the mirror would be –1.25 MPa according to the color scale. This is what we have to minimize. σ_{xx} is displayed on figure 3 given in annex.

3.3 Experiments on the ears:

3.3.1 Experimental set-up:

Since we didn't have enough time, we only tested the first Glasgow design (old one).

The idea was to bond the ear on a piece of fused silica glass, to clamp this piece and then to suspend a few masses to the fibers. Using a polariscope (described later in 4.1), we could then observe the stress distribution in the bond and especially, the stress normal to the bond layer.

The first thing was to bond the ear to the glass using the same solution described in the first part of this report. Once the bonding done, we took a picture of it:

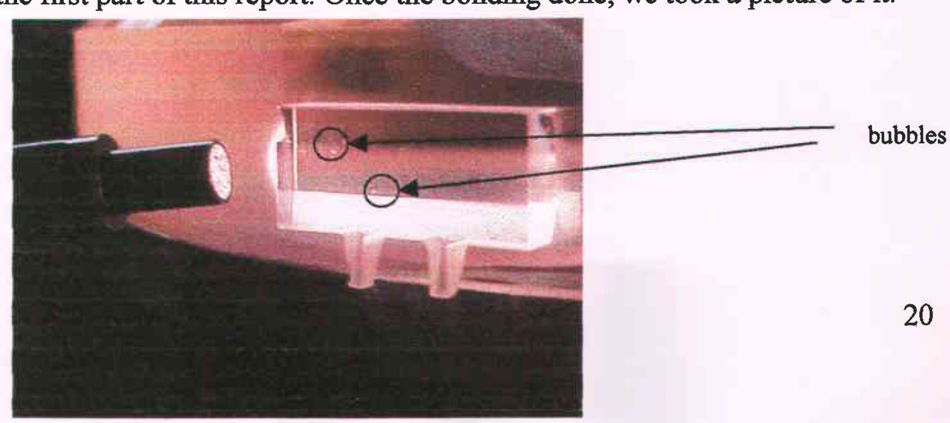

The few bubbles observed after the bonding could be dangerous as they represent stress focus points.

Then, we had to weld the fibers. Once the fibers welded, we had to organize an experiment set-up so that we could use the polariscope to visualize the stress distribution. The final set-up looks like this:

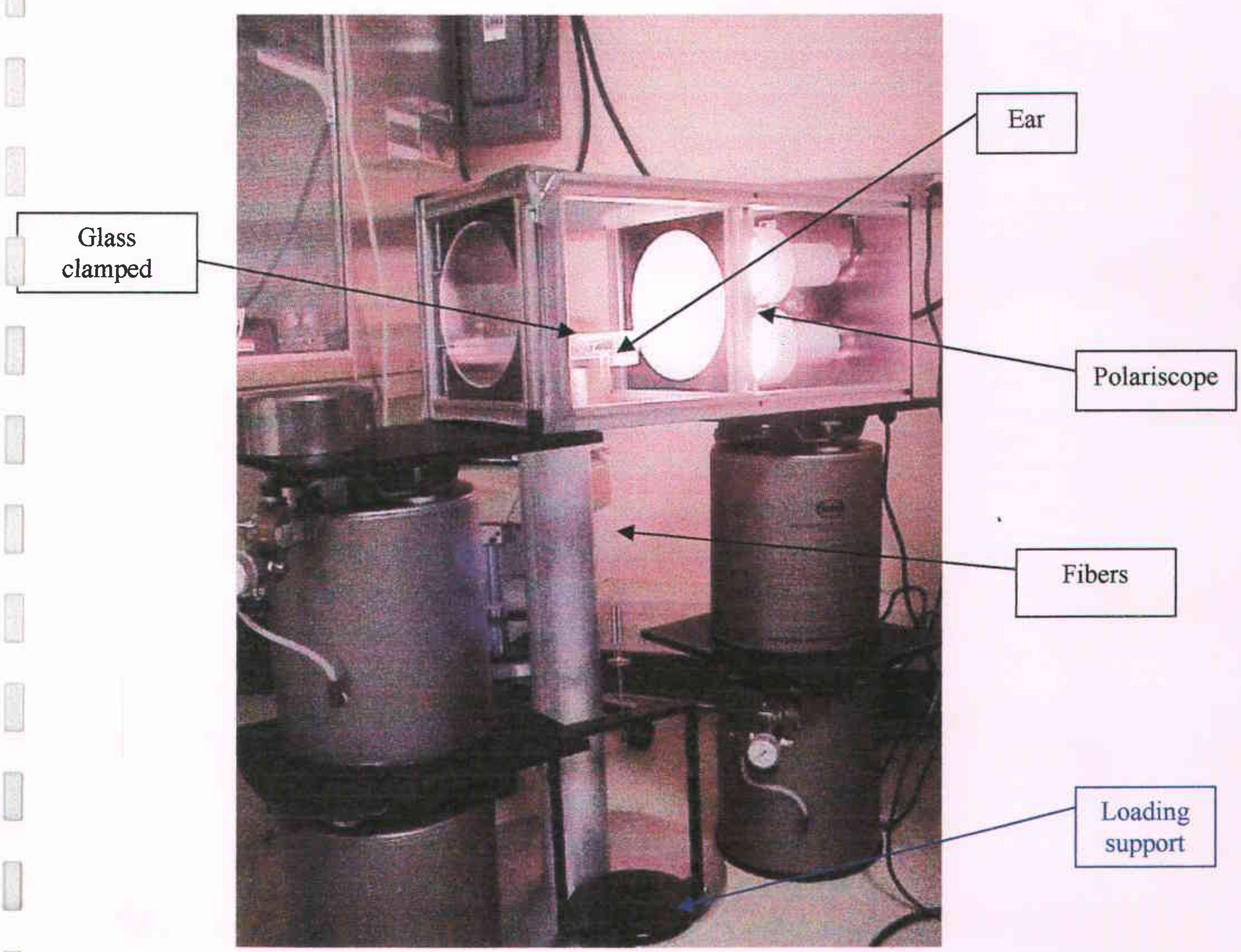

The loading support was machined especially for these experiments; the system is directly glued on the fibers:

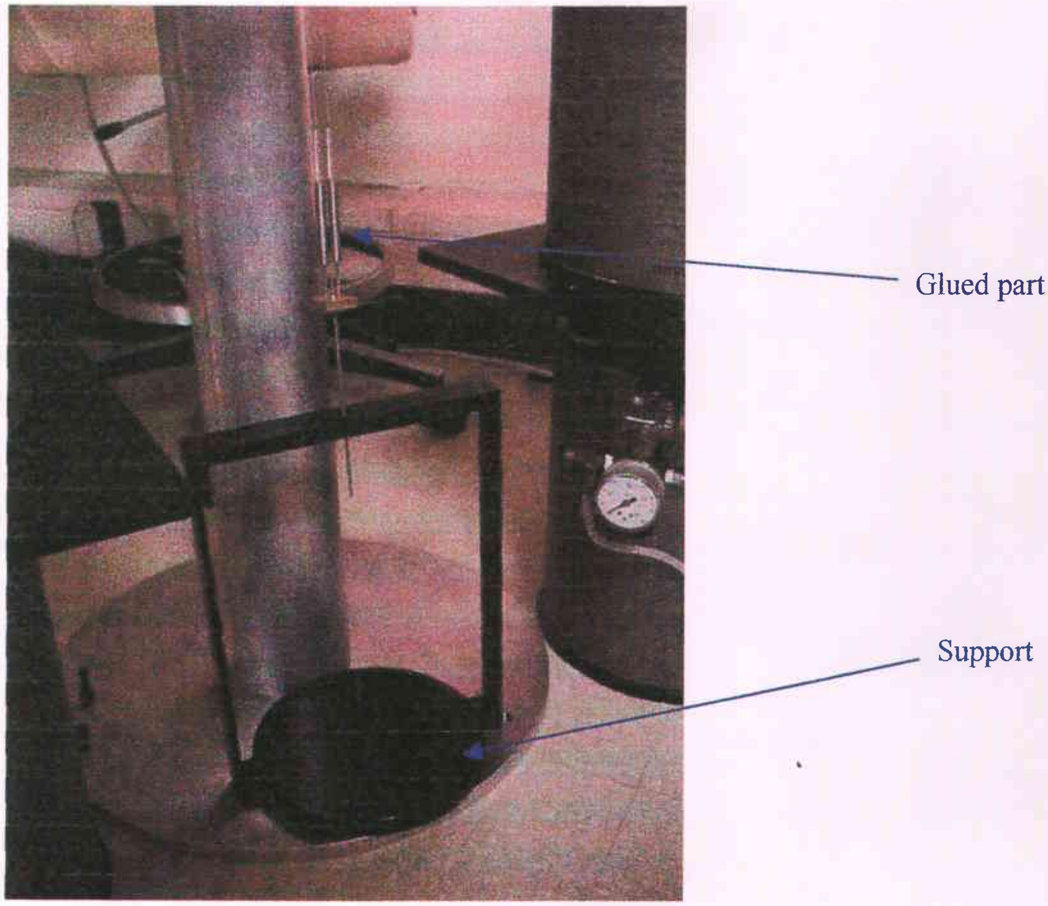

3.3.2 Results:

Without any load, not even the support, we could already see a stress distribution such as this one:

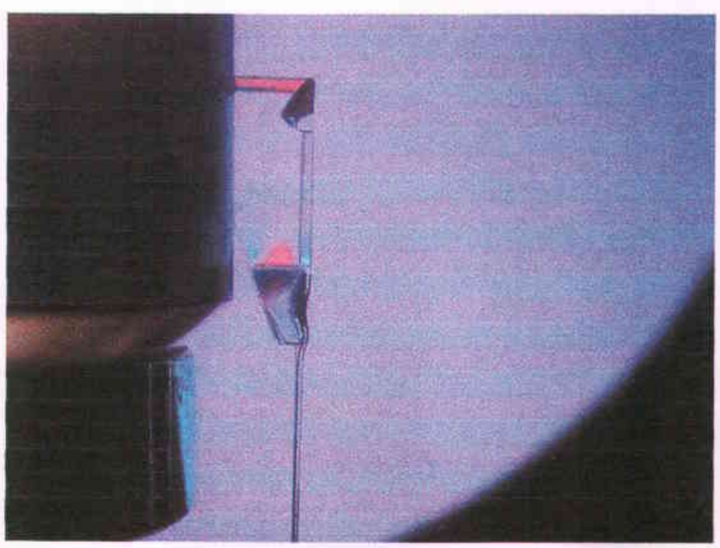

We can already see several color spots where we expected stresses focuses when loading the fibers a little more. Most of these spots are due to the geometry of the bond, especially at different edges and corners of the ear because of geometry angles.
Let's have a look to a few pictures of the stress distribution from the start to the end of the experiment:

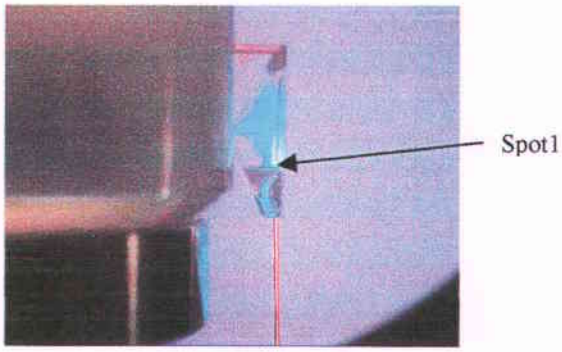

The support already weighs about 2.5 Kg by itself, which first applied a small load to the bond. When loading the fibers only with this support, we could see the stress distribution besides in the plan orthogonal to the bond through the tint plate of the polariscope.

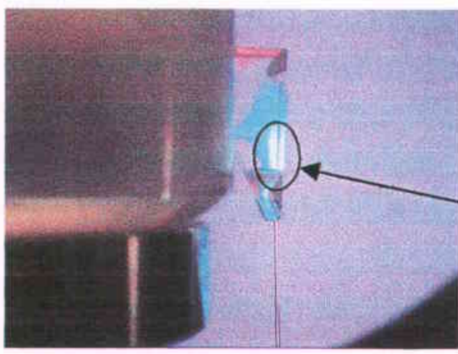

Then, we add two more kilograms to the fiber and the stress distribution started being really meaningful. All the color spots started growing very quickly, especially the yellow one we can see on the right of the ear.

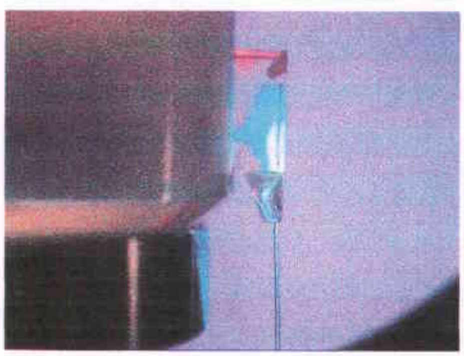

Here we can notice how the fibers are passing from red to blue according to the tension much higher than the beginning.

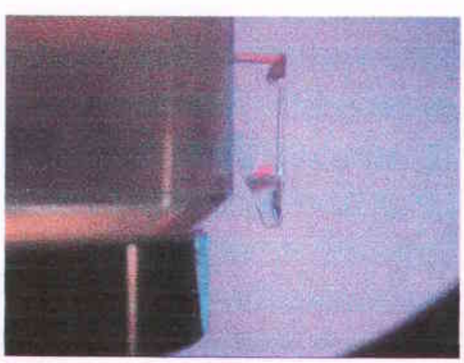

About 5 seconds after, the fibers breaks. Actually, the corresponding leg of the ear also breaks in the same time. The shape of the ear breaking reveals us the shape of the stress distribution itself.

To try to figure out the reason of the breaking, let's compare a picture of the experiment just before the breaking and the stress distributions given by Algor in the same plan:

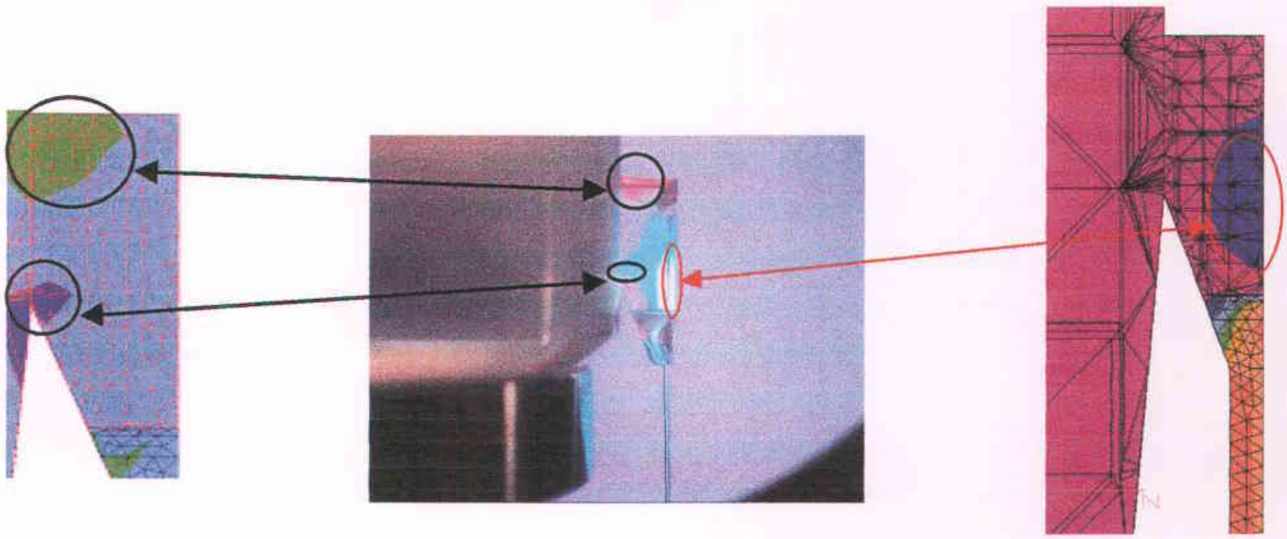

Sigma zz (Algor) | Polariscope | Sigma xx (Algor)

The different focus points observed with "Algor" can also be clearly noticed with the polariscope. Both stress distributions observed with the polariscope and displayed by "Algor" are quite similar. Hence, we can say that the FE modeling was close to the reality. Even if we didn't have time to quantify it with the polariscope, we also can assume that the stress values computed by the software can be trusted and analyzed.

Since these experiments confirms the modeling results, we will be able to use this tool to test any kind of design.

To give an explanation using the FE model, let's know have a look to the broken part of the ear:

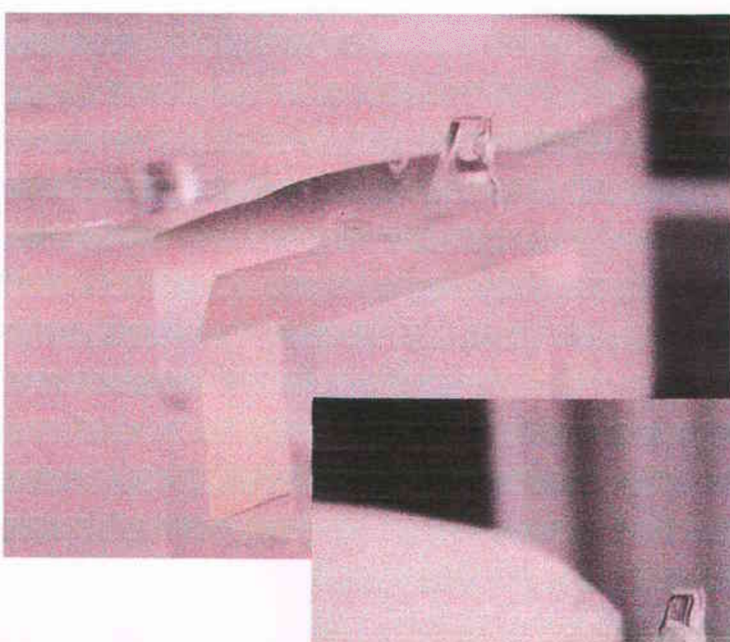

The picture besides shows very well that the ear is missing. The breaking shape can be displayed in a better way by the second picture above.

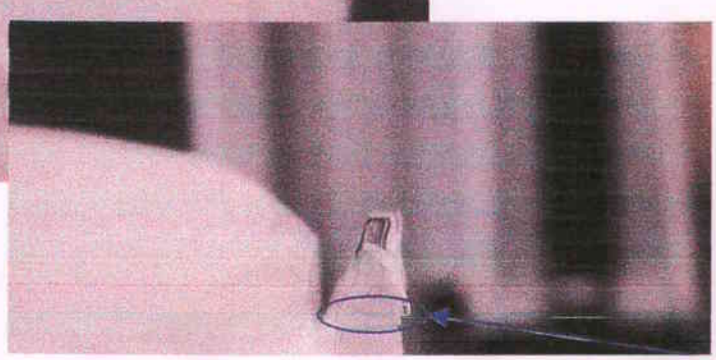

The parabolic shape of the breaking curve corresponds to the Sigma xx distribution displayed before using the software. This view of Sigma xx reveals stress focus points explaining the reasons of the breaking place:

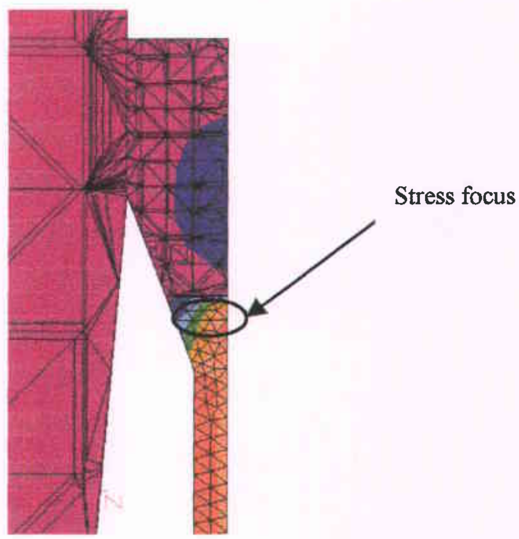

These experiments appeared as very meaningful in the understanding of the suspension behavior. We were able to determine the main reasons of the breaking and most of all, we confirmed the results computed by the software. This means that the model is useful and that we can consider the last results as close to reality.

3.4 Second bond model (Glasgow new design):

3.4.1 Suspension design:

As we introduced the mirror and the fibers before, we'll only present the ear's design and the assembly in this part.

- Ear design:

Here again, this ear was machined in Glasgow; this is their last ear design (see Figure 4 in annex):

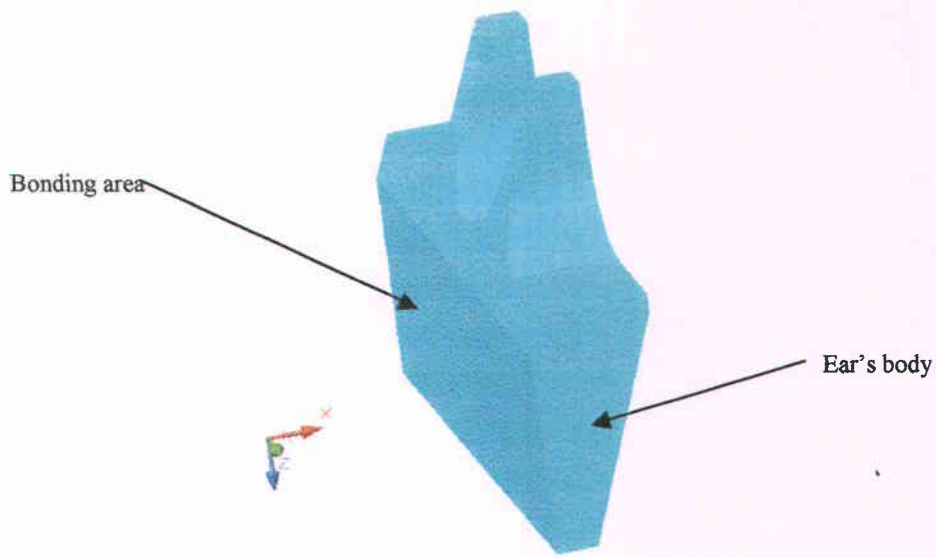

The main difference with the previous design is the trapezoidal shape of the ear's body instead of a prism shape.

- Assembly design:

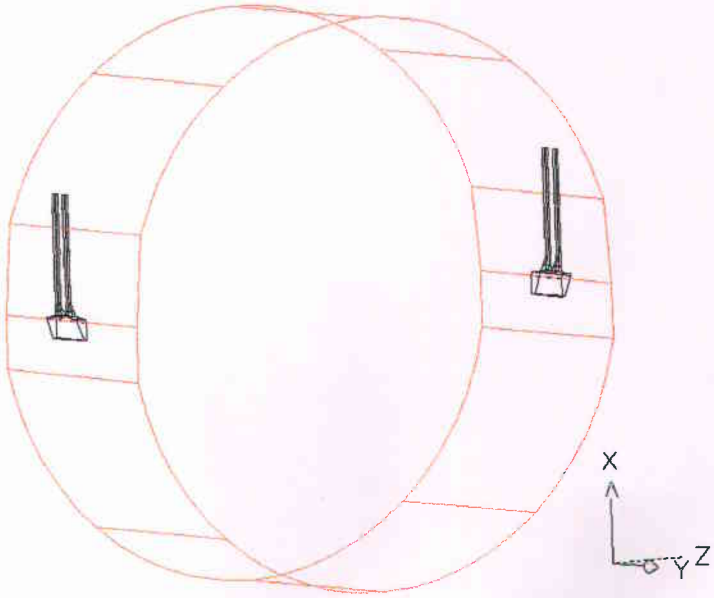

3.4.2 FEA:

The elements used for the 2-D and 3-D meshing are exactly the same that before. We also consider here the fibers as prisms with a 4 mm^2 square section.

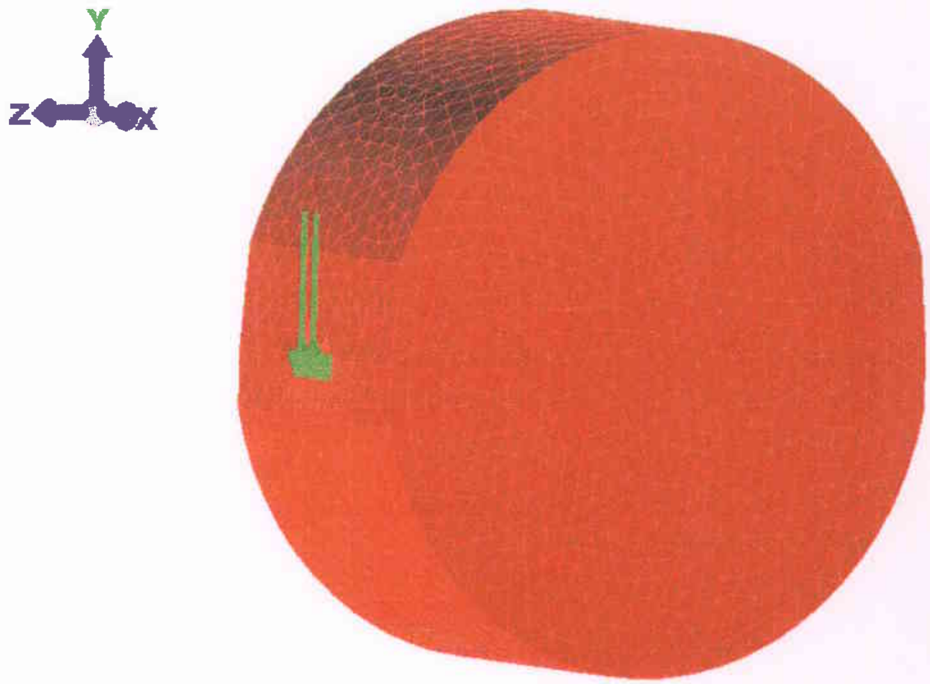

The mesh has been refined exactly the same way as for the old design, so are the assumptions (boundary conditions, load, material properties...) for the FEA. The display of shear distribution at the surface is the following one:

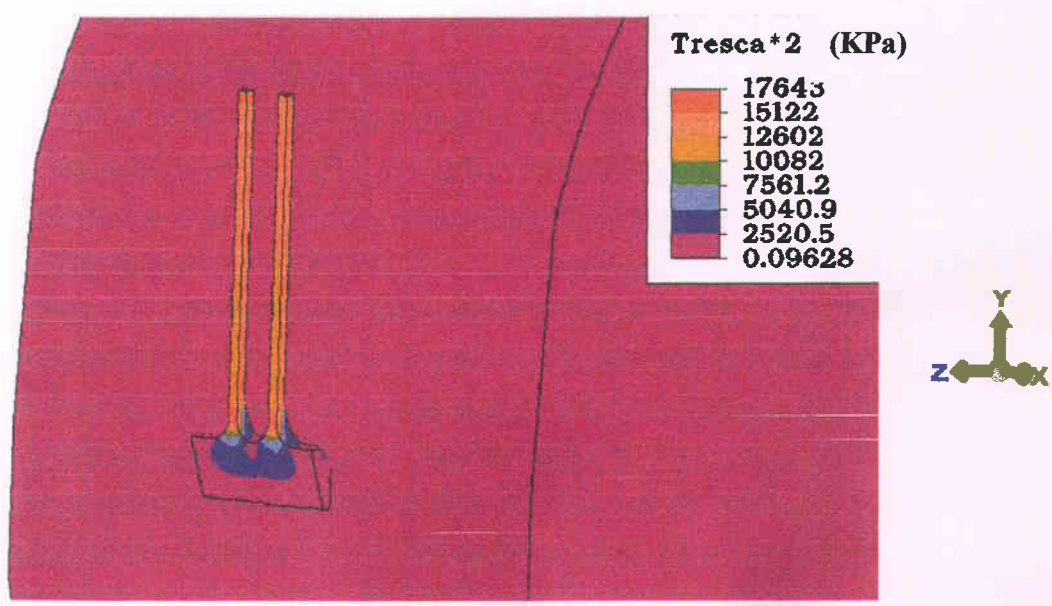

The distribution is not displayed for the whole suspension, as it's exactly the same on the other side of the mirror. Now let's have a look to the stress distribution in the bond:

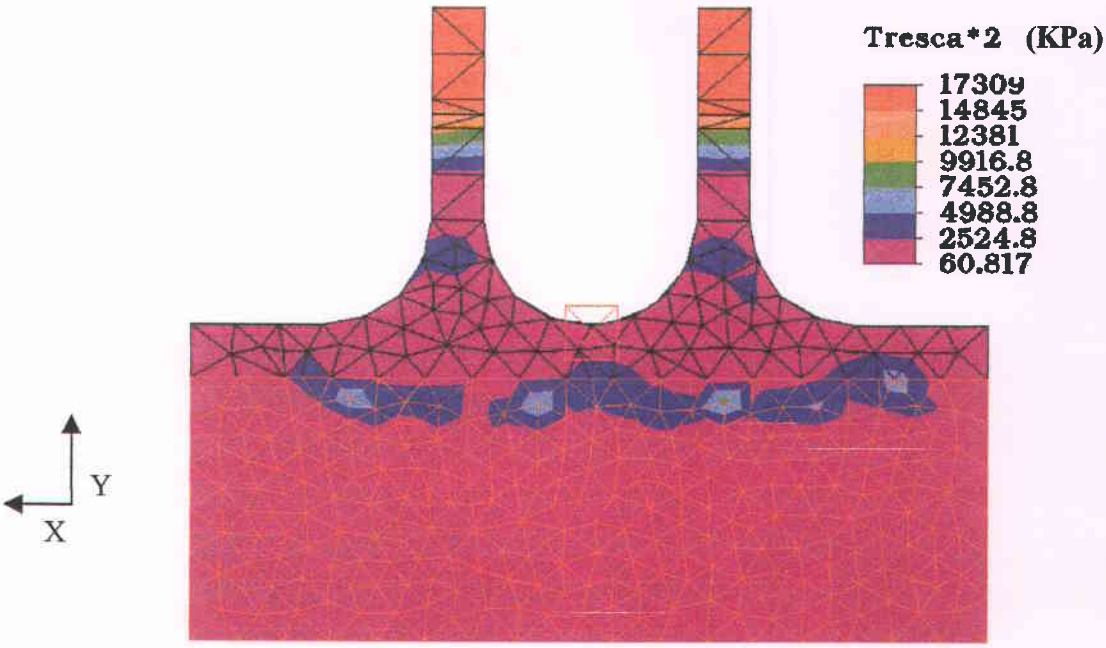

The shear distribution varies from the bottom to the top of the bond and it is vertically symmetric. Here again, the maximum shear stress (about 3.7 MPa) in the bond is very low compared to the breaking stress of this layer. We can note some stress focus points (in bright blue) at the upper limit of the bond area, which is the most sensitive part to the shear in the bond. The maximum stress is situated at the welded part of the legs. σ_{yy} is displayed on figure 5 given in annex.

Let's display the stress normal to the bond:

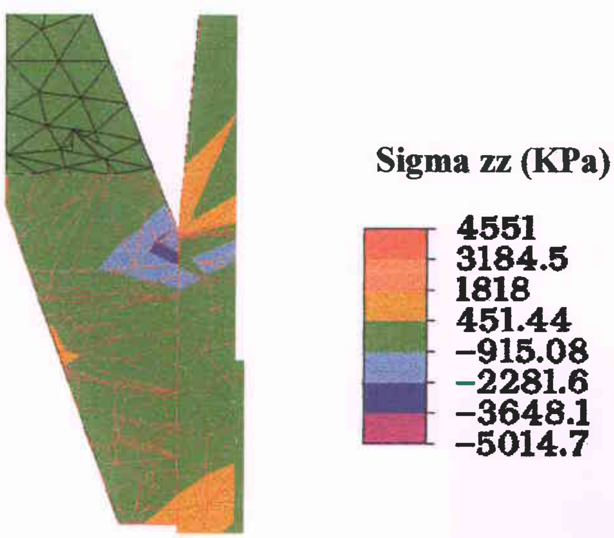

It seems like the stress applied by the mirror on the ear is larger now, especially regarding to the compression (blue colors). According to the color scale, we can estimate the maximum compression stress at –3.65 MPa.

3.5 Third bond model (LIGO design):

This paragraph will introduce the first of the two ears entirely designed in our laboratory for the LIGO project.

3.5.1 Suspension design:

As described in the paragraph 2.4, the main criterion to consider in these designs was to reduce the length between the fiber and the mirror. To bring the ear closer to the mirror, our idea was to machine the mirror. This means that we modified the sides of the mirror. The sides wouldn't be vertical anymore. To avoid the contact between the ear and the mirror sides, we introduced a little angle to incline the sides in the opposite direction to the ear.

- Mirror design:

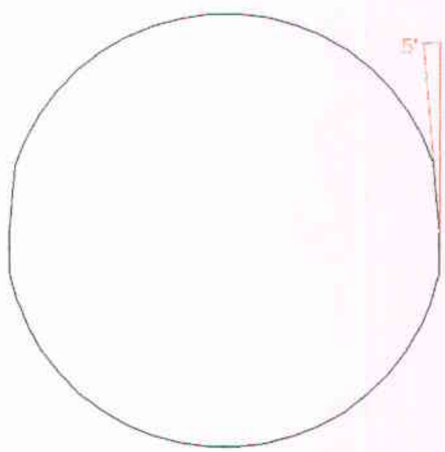

5° will be enough to avoid the contact between the ear and the mirror side but at this time, we don't know if it will be also enough to weld the fibers without damaging the mirror. Burning the mirror while welding the fibers could decrease its quality factor. Machining a larger angle won't be a problem anyway. The important thing is to keep the idea of building this inclined plane on the mirror's sides.

- Ear design (see Figure 6 in annex):

Due to the new mirror design, the bonding surface and the legs are now in the same vertical plan.

- Assembly design:

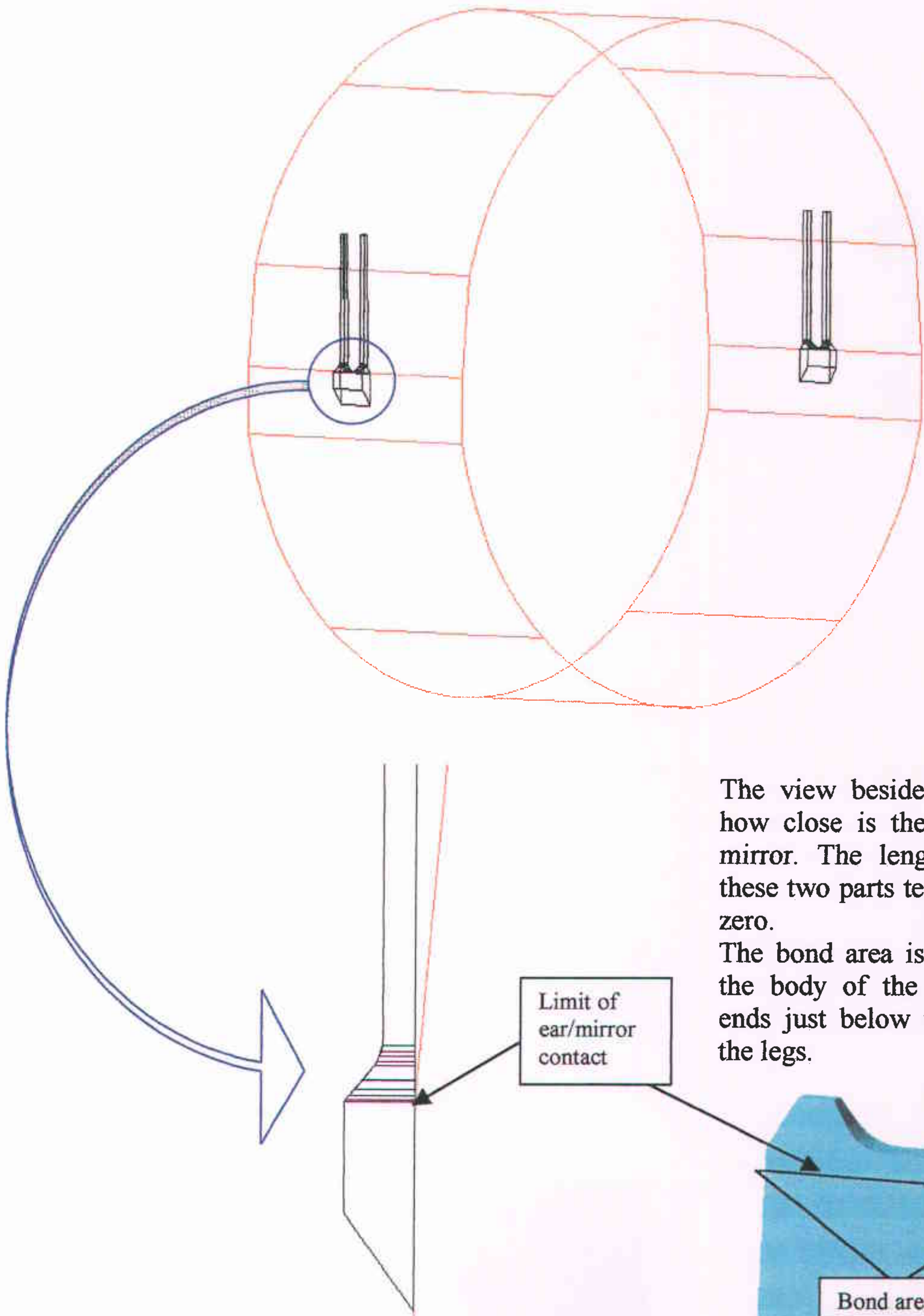

The view besides shows us how close is the ear to the mirror. The length between these two parts tends towards zero.
The bond area is defined by the body of the ear, which ends just below the base of the legs.

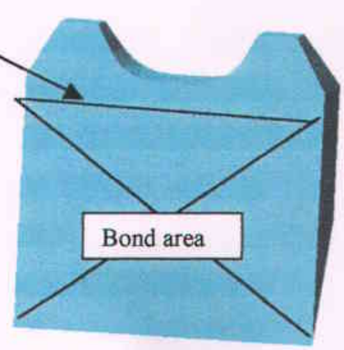

3.5.2 FEA:

The analysis is performed using the same general conditions as the two first ones, the shear distribution at the surface is:

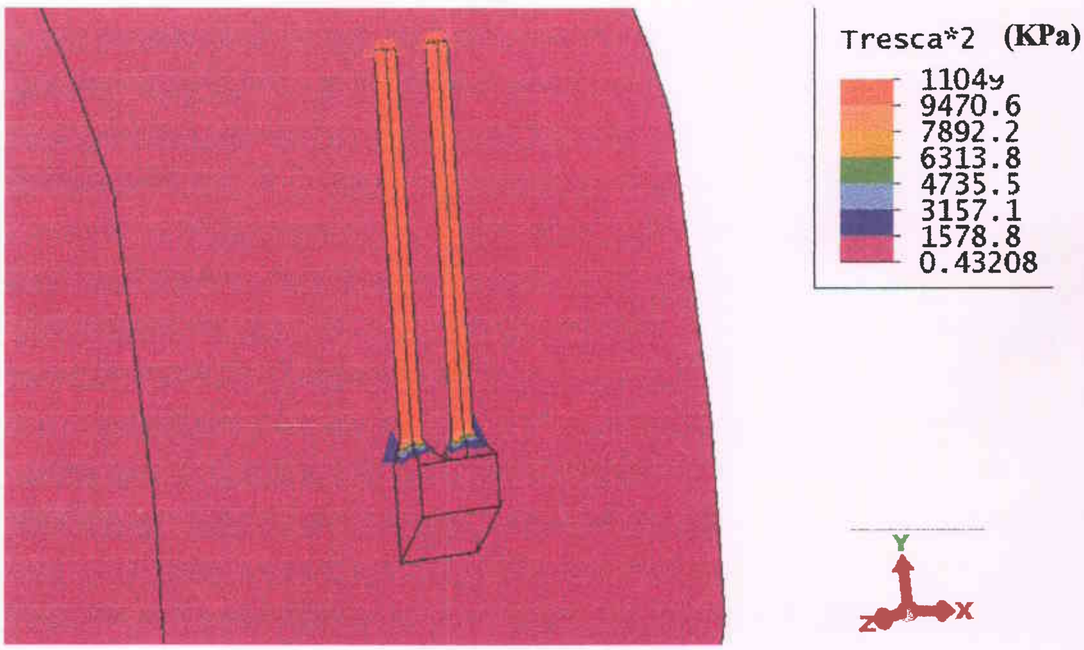

This distribution looks quite similar to the other ones, let's have a look to the bond now:

The shear in the bond looks constant. The distribution is similar to the first bond model one. The maximum shear stress is about 0.85 MPa.

Normal stress distribution:

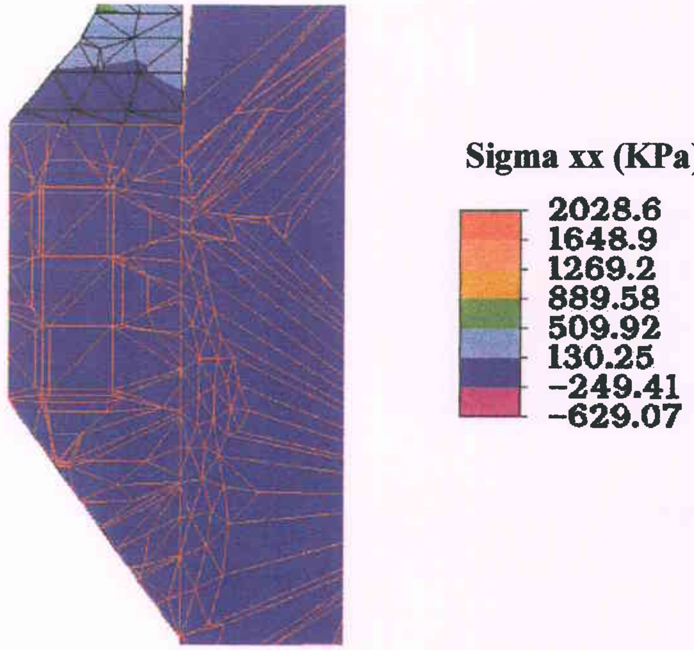

The distribution along the bond is becoming constant compared to the previous designs. The values according to the color scale are really smaller than those computed for two first ears. The mirror is not pushing and pulling the ear in the same time, we can expect shear to be the main stress in the bond now. σ_{yy} is displayed on figure 7 given in annex.

3.6 Fourth bond model (LIGO design):

Let's present and analyze the second bond designed in LIGO.

3.6.1 Suspension design:

• Ear design:

For this last design, we focused on rounded shapes; we wanted to avoid stress focus points due to small angles (see Figure 8 in annex).

This model is composed of three cones and one cylinder, and the fibers have a circular section (2mm of diameter). The mirror is machined the same that the third model one.

- Assembly design:

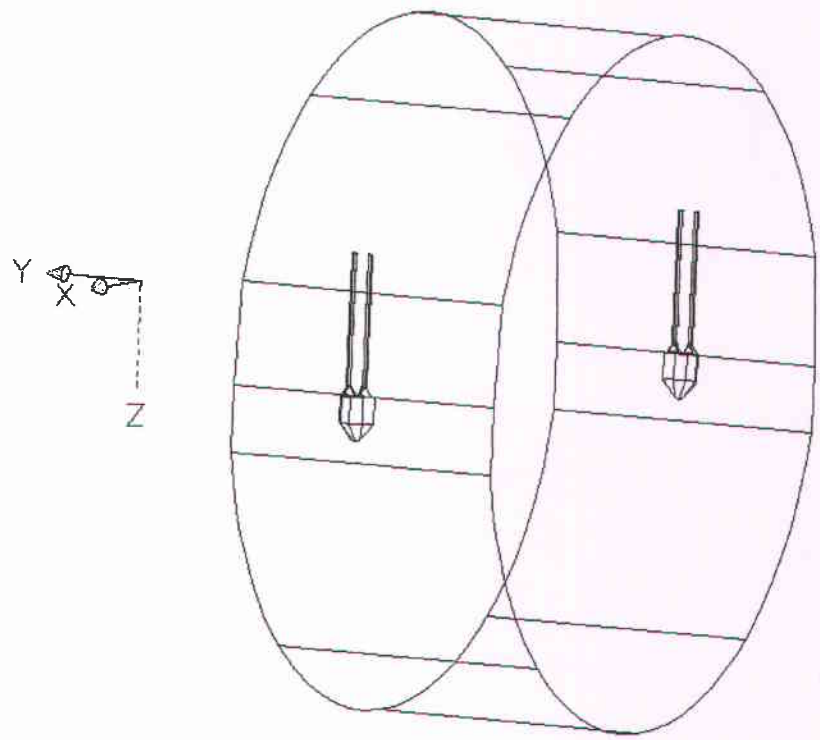

A side view of the ear upper part will allow us to display the bonding in a better way:

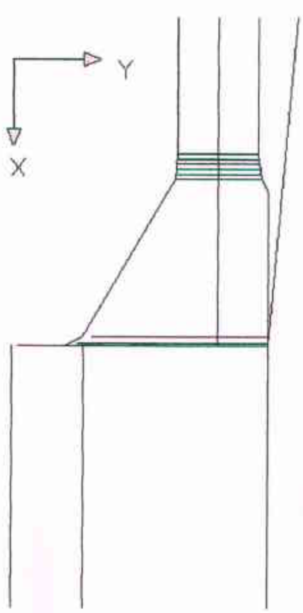

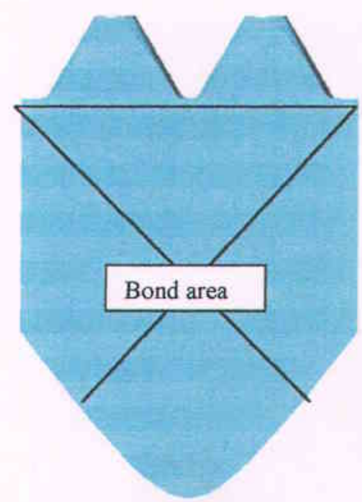

3.6.2 FEA:

Shear distribution at the surface of the bond:

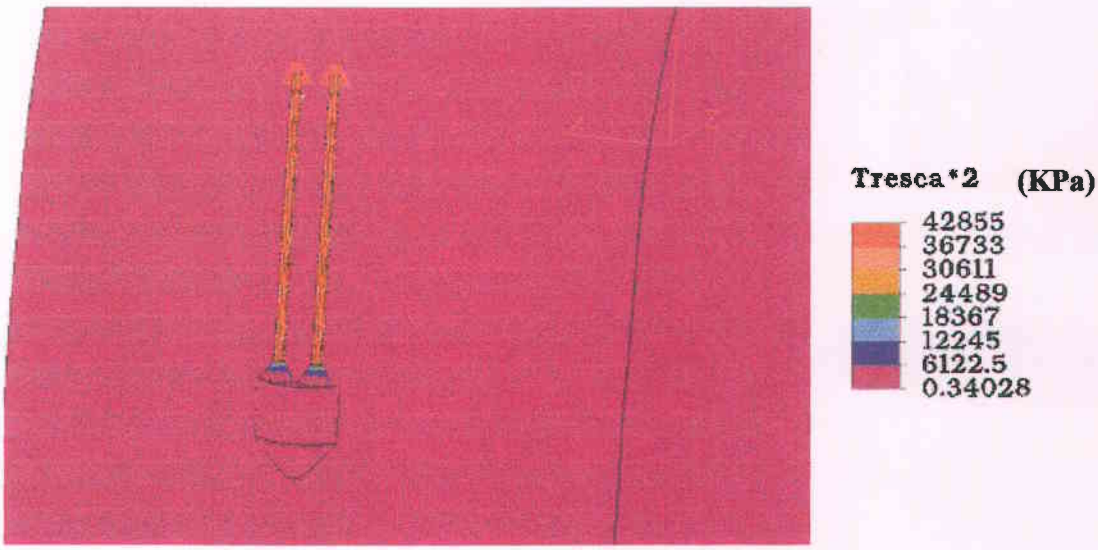

This geometry was a little more complicated to design than the other ones, let's have a look to the bond:

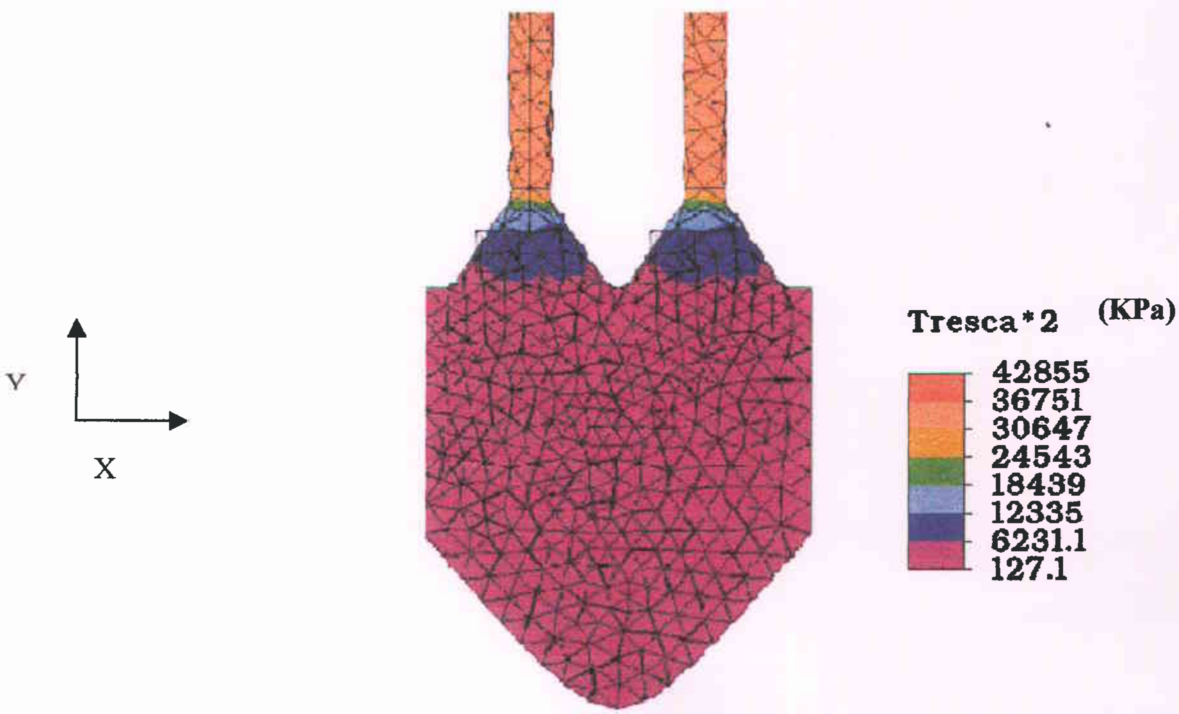

The stress distribution seems constant over the bond area. The maximum stress could be evaluated at 3.1 MPa.

Normal stress distribution:

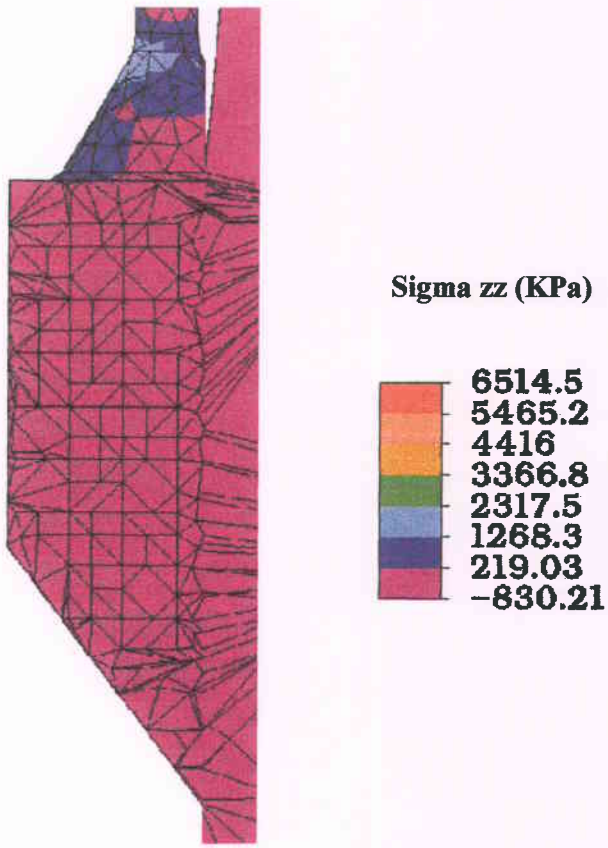

As the previous one, we are now very close to pure shear in the bond because of the geometry of the ear. The maximum normal stress is very close to zero.

3.7 Results analysis and conclusion:

To figure out which design would appear as the best one for the suspension, we have now to resume and analyze all the data obtained before.

Let's first resume in a table the stresses values obtained for each design. This table gives the shear stress in the bond (Tresca) and the stress normal to the bond (σ_{normal}) for the four models (according to Algor's color scale):

	Design 1 (Glasgow old design)	Design 2 (Glasgow new design)	Design 3	Design 4
Maximum Tresca stress (MPa)	1.11	3.726	0.85	3.1
σ_{normal} (MPa)	-1.25 (compression)	-3.65	-0.240	-0.830

If we compare the two designed from Glasgow together, there is not any important difference in the results. The old design seems to stand as the best one even concerning the stress distribution according to the pictures given by Algor.

The design 3 brings important changings, the normal stress is so close to zero, that we can consider shear as the main solicitation in the bond. The normal stress is almost completely removed which minimize the risk of stress focus at the bottom of the bond. Hence, we can expect pure shear in the bond; since shear is well known for these designs, we will be able to control it. Moreover, the values of the shear stress are very low compared to the breaking stress of the bond (20 MPa).

The design 4 seems to behave the same way. Both values of the stresses are larger than the design 3 ones. Building a larger bond area for the design 4 could bring the shear stress down.

If we assume now that the last two designs should be more adapted to the suspension than the two first ones, we now have to wonder how to machine them easily. According to its complicated shapes, the design 4 would present difficulties to get built easily. Then, the design 3 should present less troubles referring to this criteria. This design is quite close to the two Glasgow designs already machined and tested.

4 Thermo elastic study of a Sapphire-Fused silica bond:

4.1 Interest:

As we said in the first part of this report, the LIGO II design should use sapphire to build the mirrors in order to improve the Q factor. This idea wouldn't change anything in the ear design; the main material for these parts of the suspension remains Fused silica. As these two materials don't have the same thermo elastic behavior, the real question here is to know how the stress distribution will look like if we bond sapphire to fused silica. By looking at the material properties, we can notice that sapphire has a bigger thermo elastic coefficient than fused silica. Under thermal load, the fused silica part will be constrained by the expansion of the sapphire part.

Our work is to model this phenomenon where the heat behaves as a fluid going from the mirror (sapphire) to the ear (fused silica). We have to display the fact that the sapphire applies constraint to the fused silica and then, we will try to figure out if the material flow causing deformations at the bond interface of the both parts is visco elastic or plastic.

The model used for this study is very simple, it's composed of two identical cylinders bonded one to another:

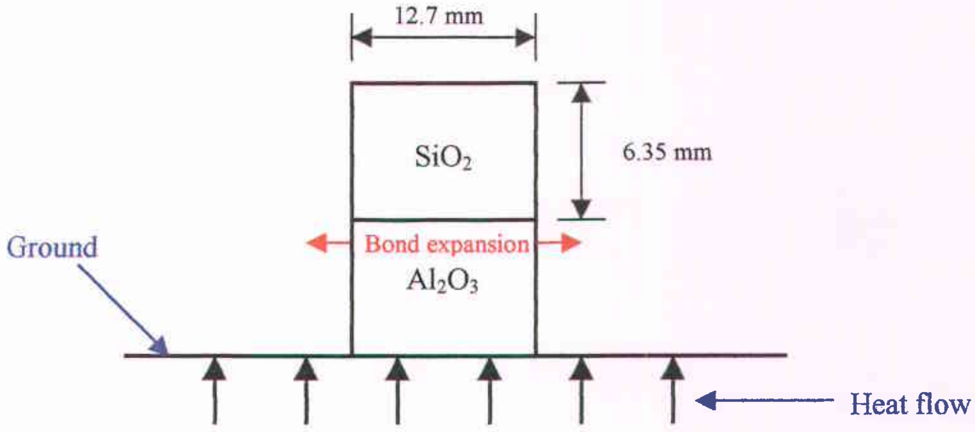

The heat source is placed under the ground so that the flow goes towards the sapphire first and then through the fused silica. Since the model is symmetric, we can expect an expansion of both parts such as the one drawn above in red.

4.2 FE modeling:

Let's model this bond using finite elements to display the stress distribution through the bond and to plot also the deformed shape.

This model is built using "Ansys" . the two cylinders are glued one to another, they are sharing the same surface at the interface. The model is meshed using tetrahedral elements and the mesh is quite fine at the lateral surface:

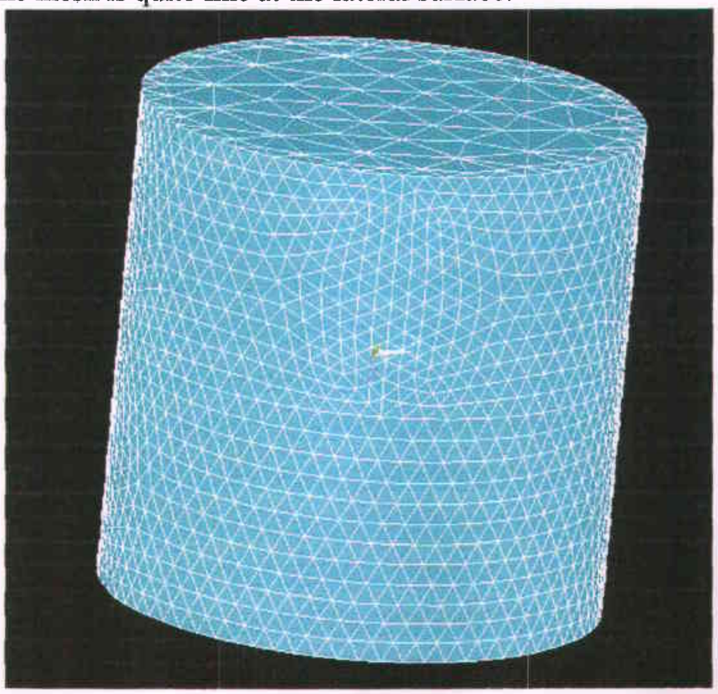

To model a thermoelastic analysis with "Ansys", we will perform a static linear analysis and we will apply a thermal load. The load is a uniform temperature applied to the whole design since we are only interested in the stress distribution at a constant temperature for the moment. We also have to give the reference temperature equal to the room temperaure (25C). By specifying the thermoelastic coefficients for both materials, the code will compute the stress distribution for a precise temperature of the bond. As a boundary condition, the translation along z is not allowed.

After a short time of calculation, for a bond at 40°C, we obtain the following stress distribution:

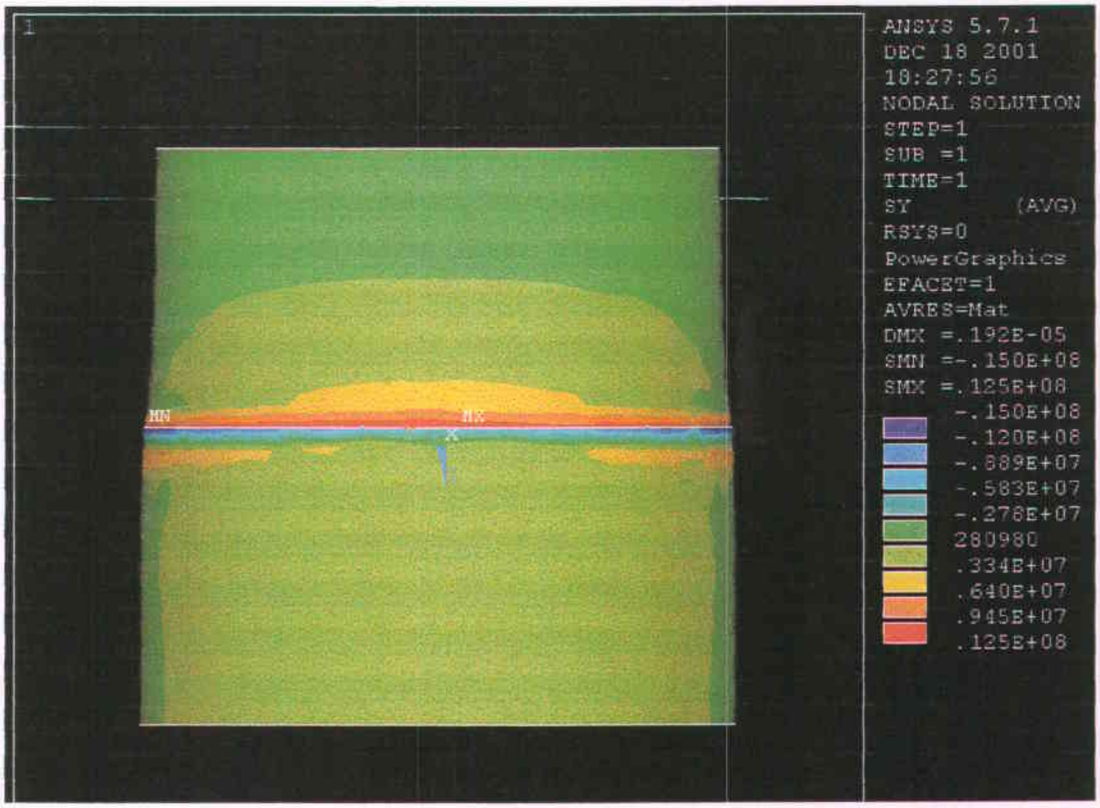

As we expected, the maximum stress is situated at the interface. The deformed shape reveals that the sapphire is applying stress to the fused silica; we can notice that the sapphire guides the deformations of the fused silica.

Concerning the stress distribution, it seems that the stress is focused right in the middle of the bond. At least, this is what we can observe for the stress along Y, where Y comes out of the screen. Let's have a look of the stress in the x direction, which is still in the plane of the bond:

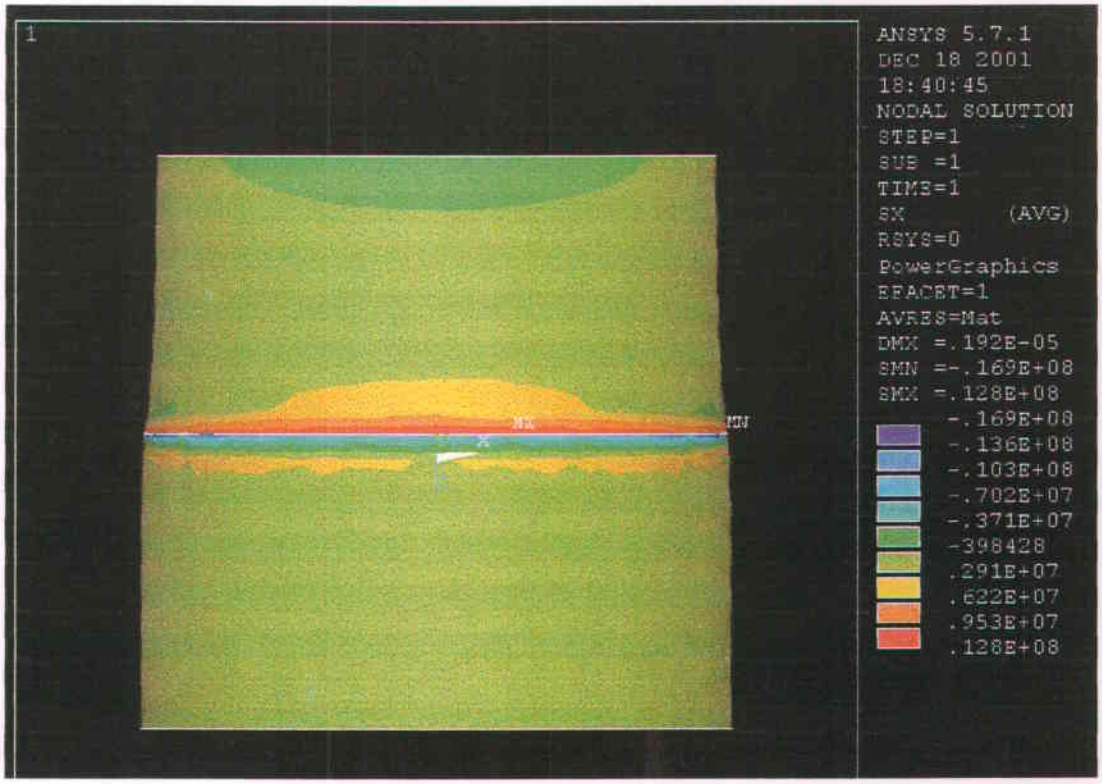

The distribution looks quite the same than before which seems consistent as the model is symmetric along z.

4.3 Experiments:

Now, we have to check our FE modeling by comparing the results to experiments ones. With special apparel called Polariscope, we are going to observe the stress distribution through the bond.

4.3.1 Polariscope principle [4]:

Here is a simple sketch of a plane polariscope principle:

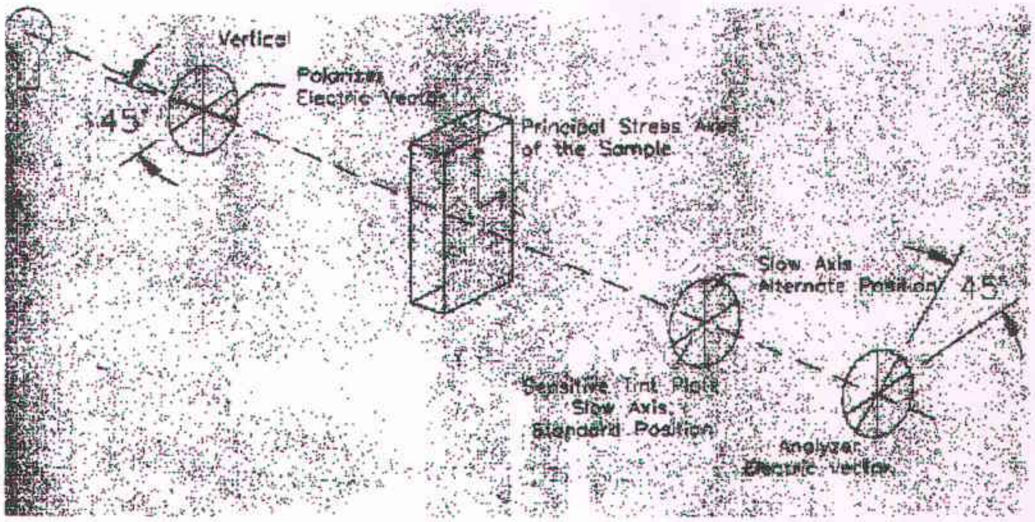

As polarized light propagates through strained glass or plastic, it experiences a retardation (between the two polarization components of the light) proportional to the amount of stress. A Polariscope (or Photoelastimeter) is an instrument, which can be used to qualitatively view and/or quantitatively measure this retardation according to a color scale. The stress distribution is displayed through the glass of the sample by isochromatics. Stress can be calculated knowing the amount of retardation, length of the light path through the sample, and the birefringence (stress optical) constant of the sample. The relation between these several parameters is the following one:

$$\delta = \frac{2\pi h}{\lambda} \times C \cdot t \cdot (\sigma_1 - \sigma_2) \qquad (1)$$

Where: δ is the amount of retardation (function of a color scale specified in the apparel manual),

λ is the wavelength of the light used,

C is the birefringence constant of the sample (fused silica),

t is the thickness of the sample where the stress is measured,

σ_1 and σ_2 are the stresses in the two first principal stress directions of the sample.

4.3.2 Experimental set-up:

We can begin by having a look to the set-up we used for these experiments:

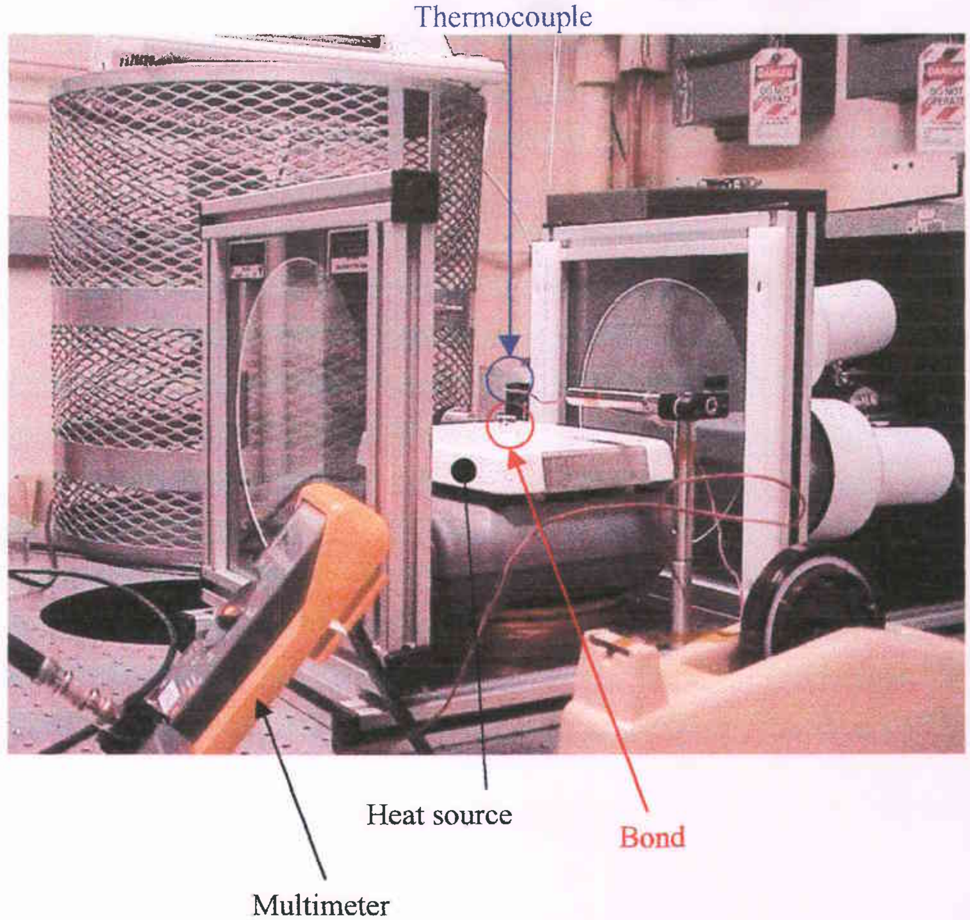

A plate generates the heat so that the flow goes through the sample from the bottom. This plate can heat the sample up, cool it down or maintain it at a constant temperature. The thermocouple is in contact with the top of the sample, its voltage varies with temperature. This voltage is transmitted to a multimeter, which will convert it into a temperature in degrees Celsius.

This test on the sample will inform us about two things: the stress distribution in the bond at a certain temperature and the nature of the flow. We can quantify the study by evaluating $\sigma_1 - \sigma_2$ and compare it to the FEA results for a certain temperature. The nature of the flow will depend on the evolution of the stress distribution with time. If this is a viscoelastic flow, the stress distribution will keep changing from room temperature to the highest temperature and in the opposite way when we cool the sample down. If it's a plastic flow, for a precise temperature, as we reach the plastic domain of the glass, the stress distribution will freeze and will remain the same even if the temperature changes.

Then, to figure out the type of material flow in the glass, we will record the evolution of the stress distribution vs. time with a camcorder. To have a very large field of data, we first heat the sample up from 24°C (room temperature) to 130°C, and then we cool it down to room temperature. Here are a few pictures of the stress distribution during heating and cooling:

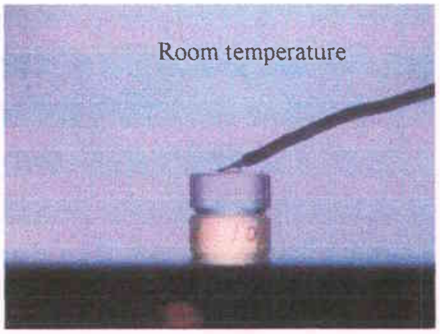
Room temperature

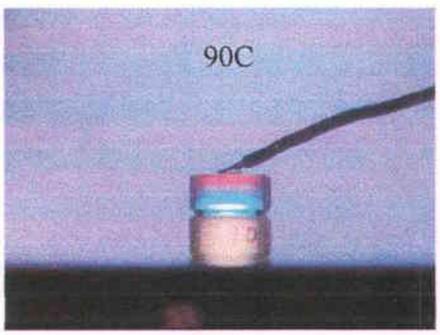
90C

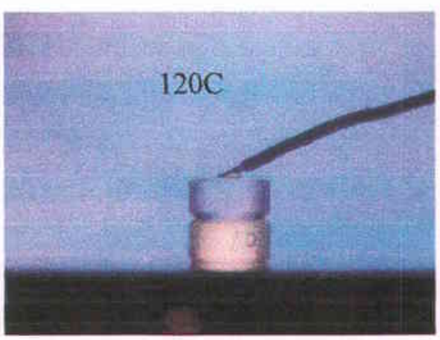
120C

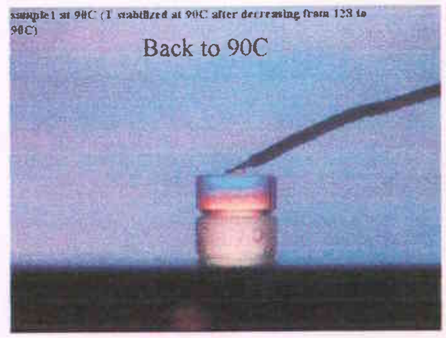
Back to 90C

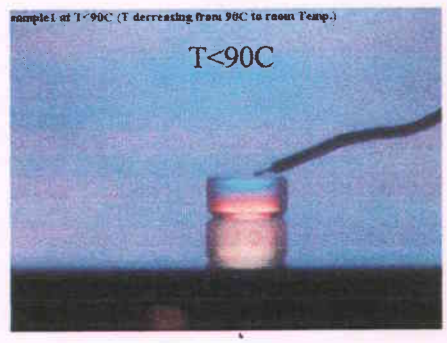
sample1 at T<90C (T decreasing from 90C to room Temp.)
T<90C

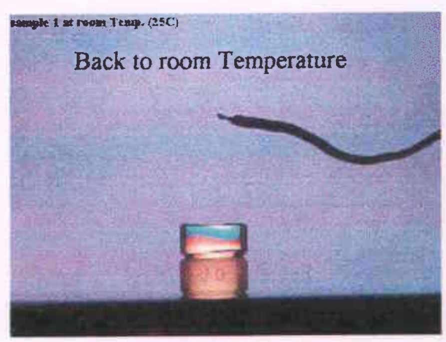
sample 1 at room Temp. (25C)
Back to room Temperature

The stress distribution is really changing during the heating of the sample. The stress is increasing until 90°C approximately and then it is decreasing until 120°C. At 120°C, the stress distribution is exactly the same as if the sample wasn't stressed at room temperature. According to these observations, we can already consider that the flow is viscoelastic since we don't have any temperature for which the distribution becomes constant.

The relaxation is more meaningful concerning the type of flow. During cooling, the sample seems to do exactly the same than during the heating but in the opposite way. The relaxation of the sapphire gives its final stress distribution to the bond at room temperature. We can definitely say that the flow is viscoelastic.

An important thing to notice is the difference of stress distribution between the beginning and the end of the experiment. This is the confirmation that viscoelasticity is more complicated than pure elasticity. We could find an explanation to this by considering the viscous properties of the bond layer. We know that viscosity decreases as temperature increases for glass. We also know that the more we add Na to the bond layer solution, the less its viscosity. So, if we assume that Na atoms are moving from the bond layer to the fused silica part during heating, it could modify the regular viscous behavior of fused silica when cooled down. That could explain why the stress distribution is so colorful when we are back to room temperature.

A viscoelastic flow could be more dangerous for the suspension than a plastic one. For a plastic flow, since we know the transition temperature, we can still try to stay below it to avoid a high amount of stress. Anyway, time won't change anything to the stress distribution since we reach the plastic domain. If the flow is viscoelastic, as we don't have any limit in temperature concerning the stress distribution, time becomes a really important factor. As the viscosity of the bond decreases with the temperature, if we apply a constant load to it, the strain will increase with time. This is the definition of creep. Then, for a very long time, the suspension of the mirror would permanently being deformed under load.

Trying to quantify the observations could be interesting. To do so, we will calculate $\sigma_1 - \sigma_2$ that we observe when the sample is back at room temperature. Then, we will compare it to the FE modeling results we obtained at several temperatures. if one of these models at a certain temperature gives approximately the same results, then we can also consider this temperature as a transition temperature in the stress distribution evolution.

4.3.3 Results analysis:

After modeling and analyzing the bond for several temperatures (from 30 to 120°C), we can easily calculate $\sigma_1 - \sigma_2$ according to the color scale of Ansys results. The values were taken at the interface Sapphire/fused silica right in the middle of the bond layer. Let's have a look to these values:

Temperature (°C)	30	40	60	90	120
σ_1 - σ_2 (MPa)	2.6	7.8	18.2	33.8	49.6

If we plot σ_1 - σ_2 vs. temperature, we obtain the following graph:

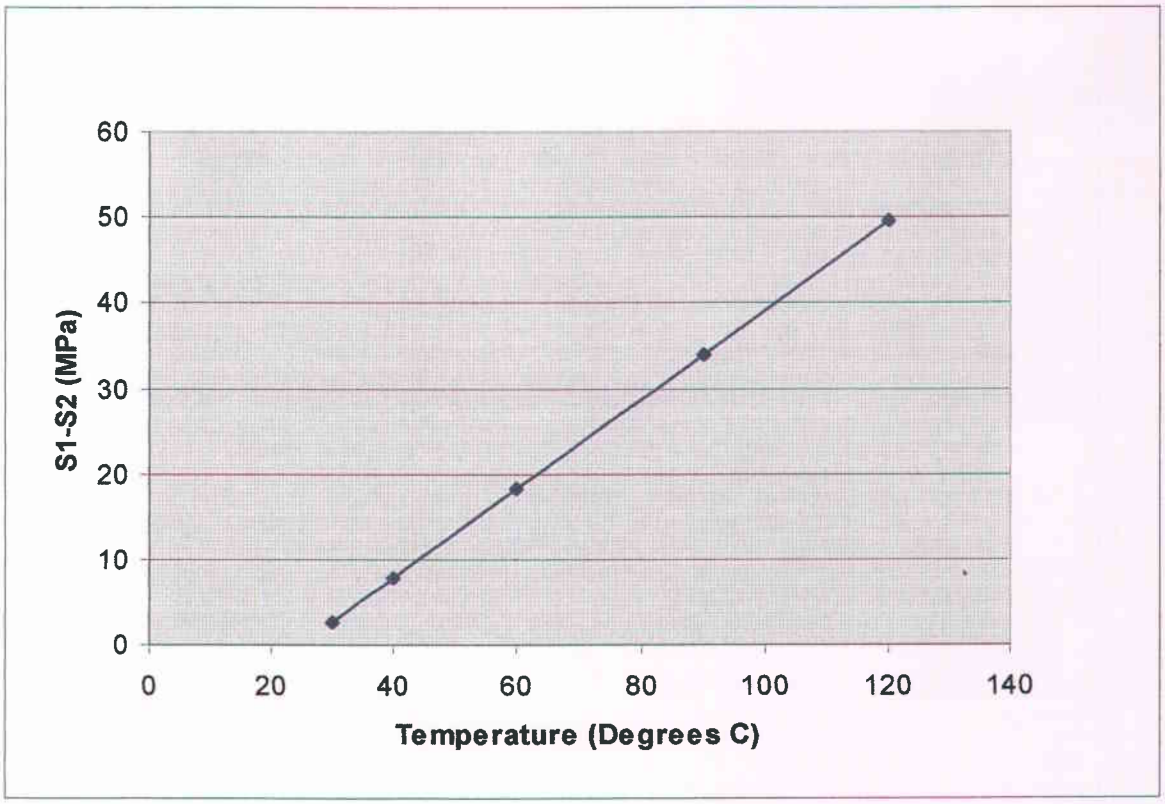

According to the viscoelastic behavior of the bond, the stress varies linearly with temperature.

We now have to calculate σ_1 - σ_2 for the bond we made the experiment on. As described before we are going to the color scale of the isochromatics to calculate the amount of retardation use and the relation (1) to determine σ_1 - σ_2. The value of σ_1 - σ_2 will be calculated at the same point we did it for the models. For this calculation, we will consider the stress distribution of the bond at the end of the experiments. In this case, we have the following parameters:

$\lambda = \lambda_{\text{regular light}} = 6.626\times10^{-34}$ J.s $= 6.626\times10^{-34}$ N.m.s
$C_{\text{fused silica}} = 3.45$ (nm/cm) (kg/cm^2) $\approx 3.45\times10^{-6}$ N/cm^2
$t = \phi_{\text{sample}} = 12.7$ mm (middle point)

and for the current sample we estimated at the end of the test:
$\delta = 270$ nm (retardation corresponding to yellow-white color).
Hence, using (1) we obtain:

$$\sigma_1 - \sigma_2 = \frac{\lambda \cdot \delta}{C \cdot t \cdot 2\pi \cdot h} \approx 9.6 MPa$$

Then if we compare this value to the results given in the table below, we can assume that the transition temperature of the bond in the stress distribution is around 40°C.

Starting from this temperature, we can consider that the viscosity of the flow really starts to act on the stress distribution. The next step to this study would be to quantify precisely the viscosity of the material flow.

CONCLUSION

The finite elements modeling revealed us interesting things about each designed we analyzed. The comparison between modeling results and experiments results allows us to say that we can be confident in the modeling. Though, regardless to research, we can not consider any of the four designs as the final solution. The best results, obtained for the designs 3 and 4, should be compared to experiments we didn't have time to perform. Then, the machining of the "ears" will also have to be studied before taking any decision. Anyway, after this work, are know able to choose the right according to the stress distribution.

The last part of the study confirmed us the nature of the material flow at the interface Sapphire/Fused silica under thermal load. Hence, we can expect creep as a new problem for the suspensions of LIGO II. These results have now to be developed by quantifying the variations of the bond viscosity with time.

In a general way, the internship at Caltech working on the LIGO project remains a good experience in the learning of new notions. Doing research in this laboratory was a real opportunity to discover another field of science and to meet very competent searchers.

REFERENCES

[1] « LIGO fundamentals », slide show, www.ligo.caltech.edu

[2] A. Bertolini, G. Cella, E D'Ambrosio, R. De Salvo, V. Sannibale, A. Takamori, N. Viboud, « Seismic Attenuation System (SAS) overview for LIGO II», internal working note, fig.1 p.3, 1999

[3] GEO suspension team, « LIGO II suspension : reference designs », p.2, 2000

[4] « Polariscope 407A41 instruction manual », Rudolph Instruments, Inc.

Figure 1

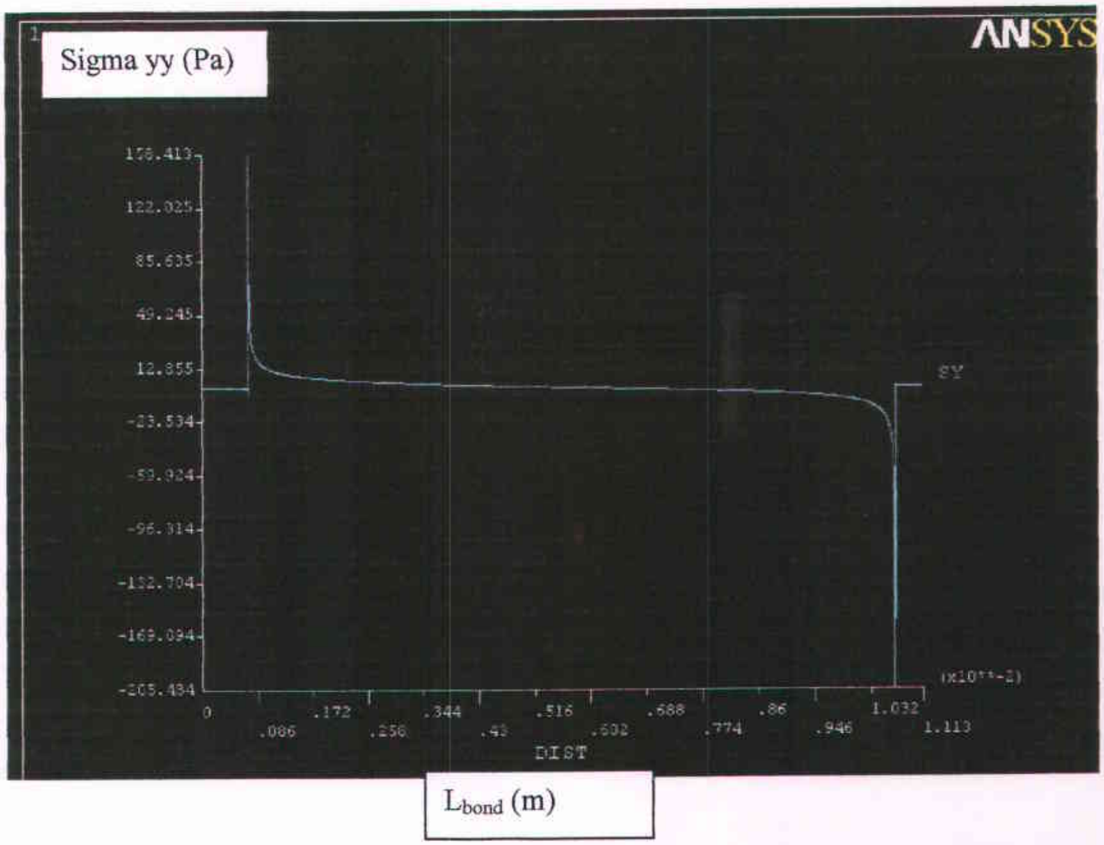
ANSYS
Sigma yy (Pa)
158.413
122.025
85.635
49.245
12.855
-23.534
-59.924
-96.314
-132.704
-169.094
-205.484
SY
(x10**-2)
0
.086
.172
.258
.344
.43
.516
.602
.688
.774
.86
.946
1.032
1.113
DIST
Lbond (m)

Figure 2

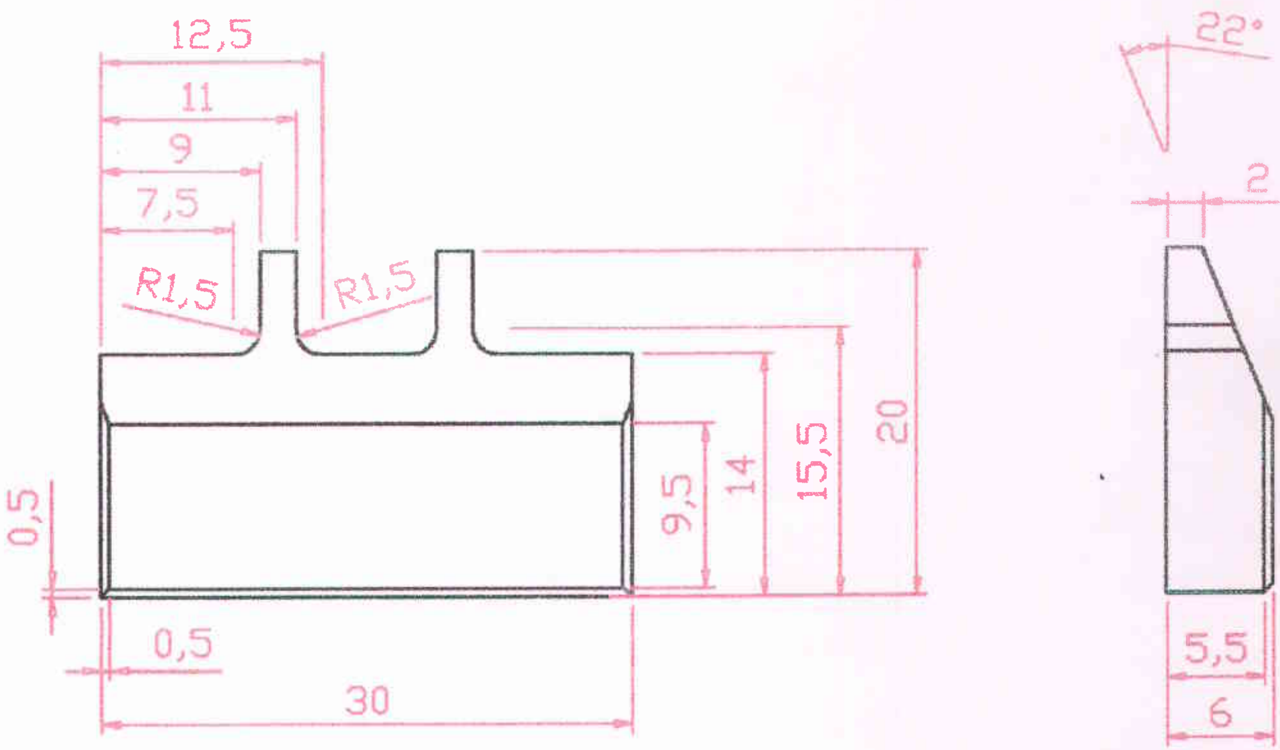

Figure 3

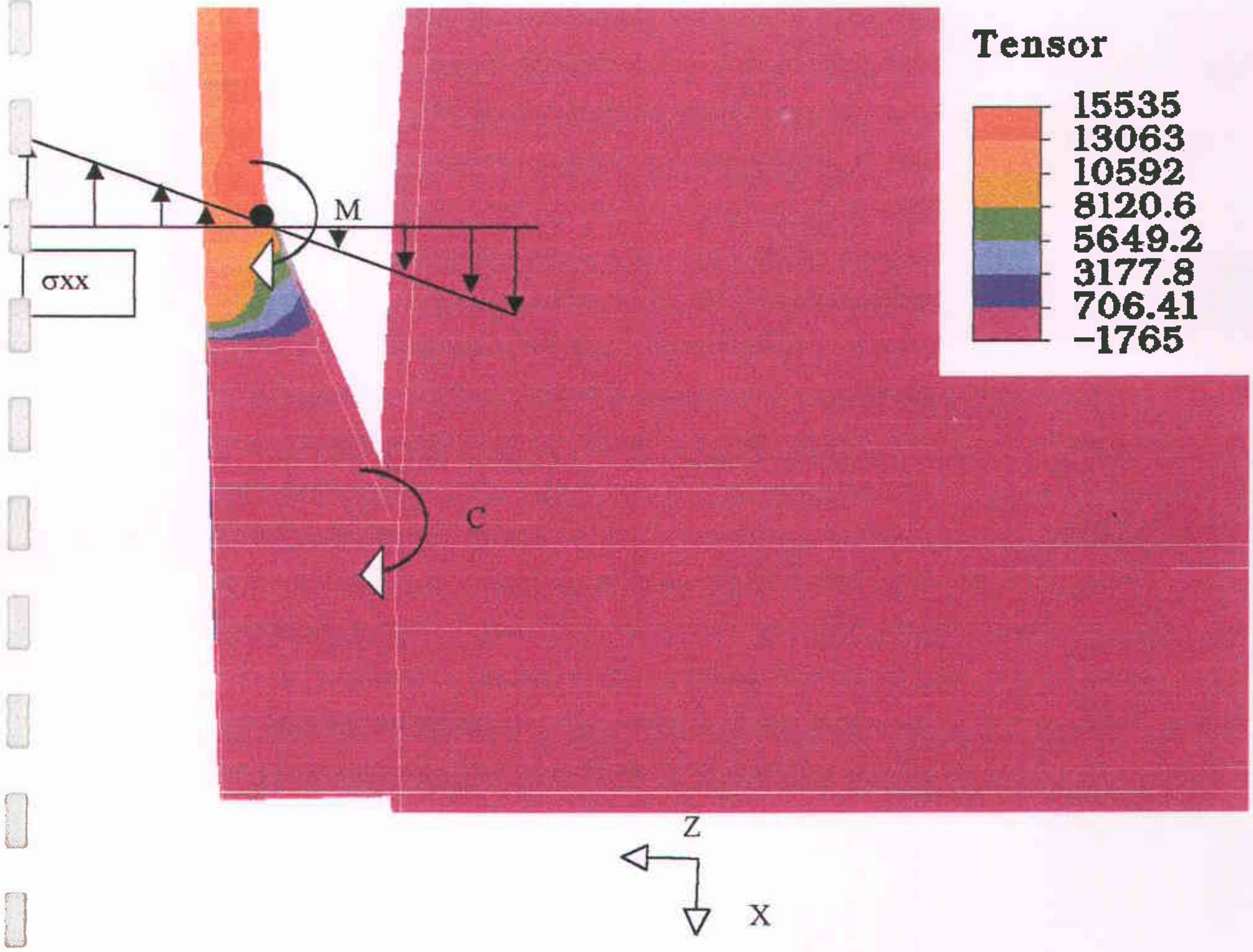
Tensor
15535
13063
10592
8120.6
5649.2
3177.8
706.41
-1765
M
σxx
C
Z
X

Figure 4

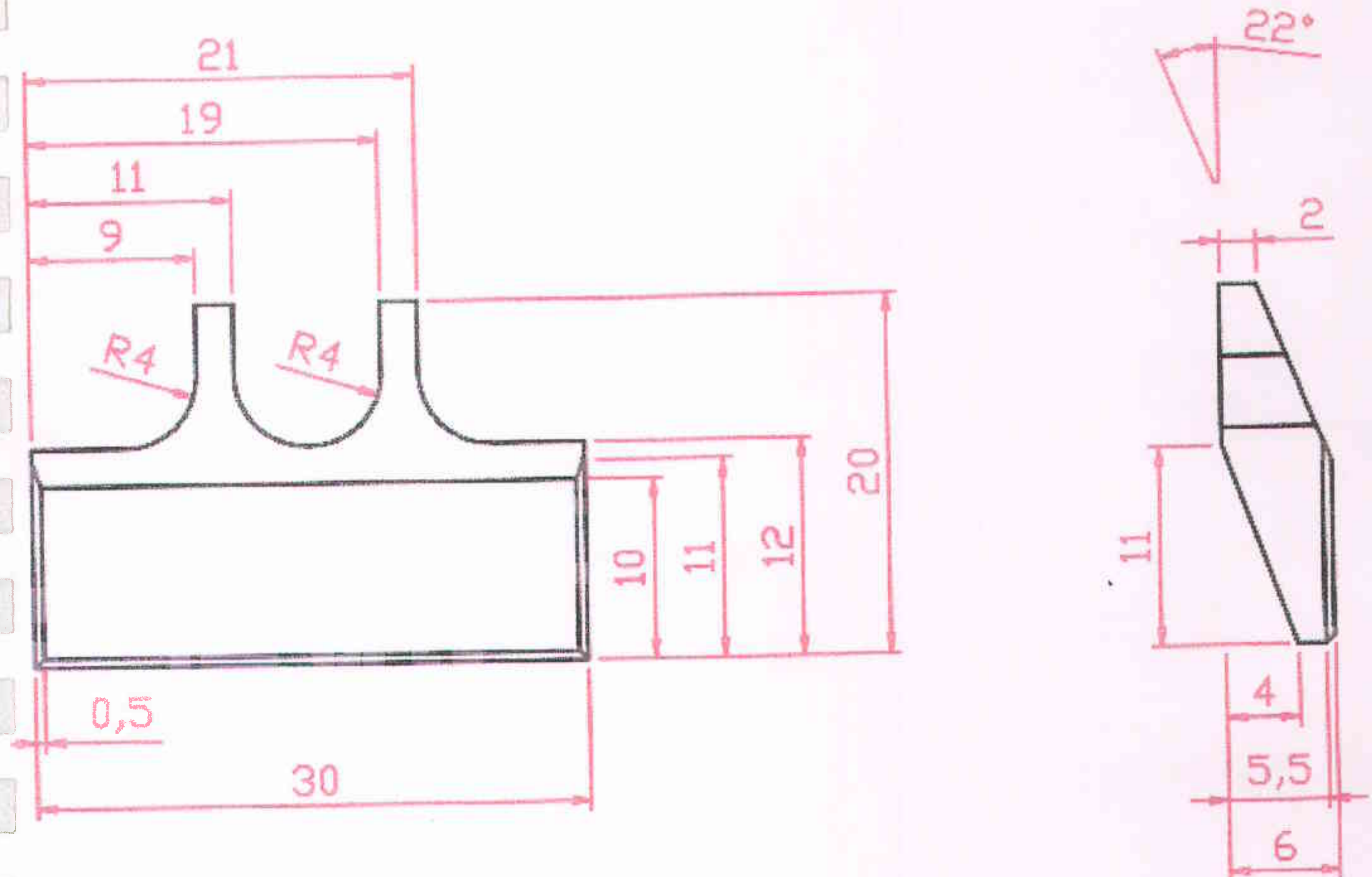

Figure 5

Figure 6

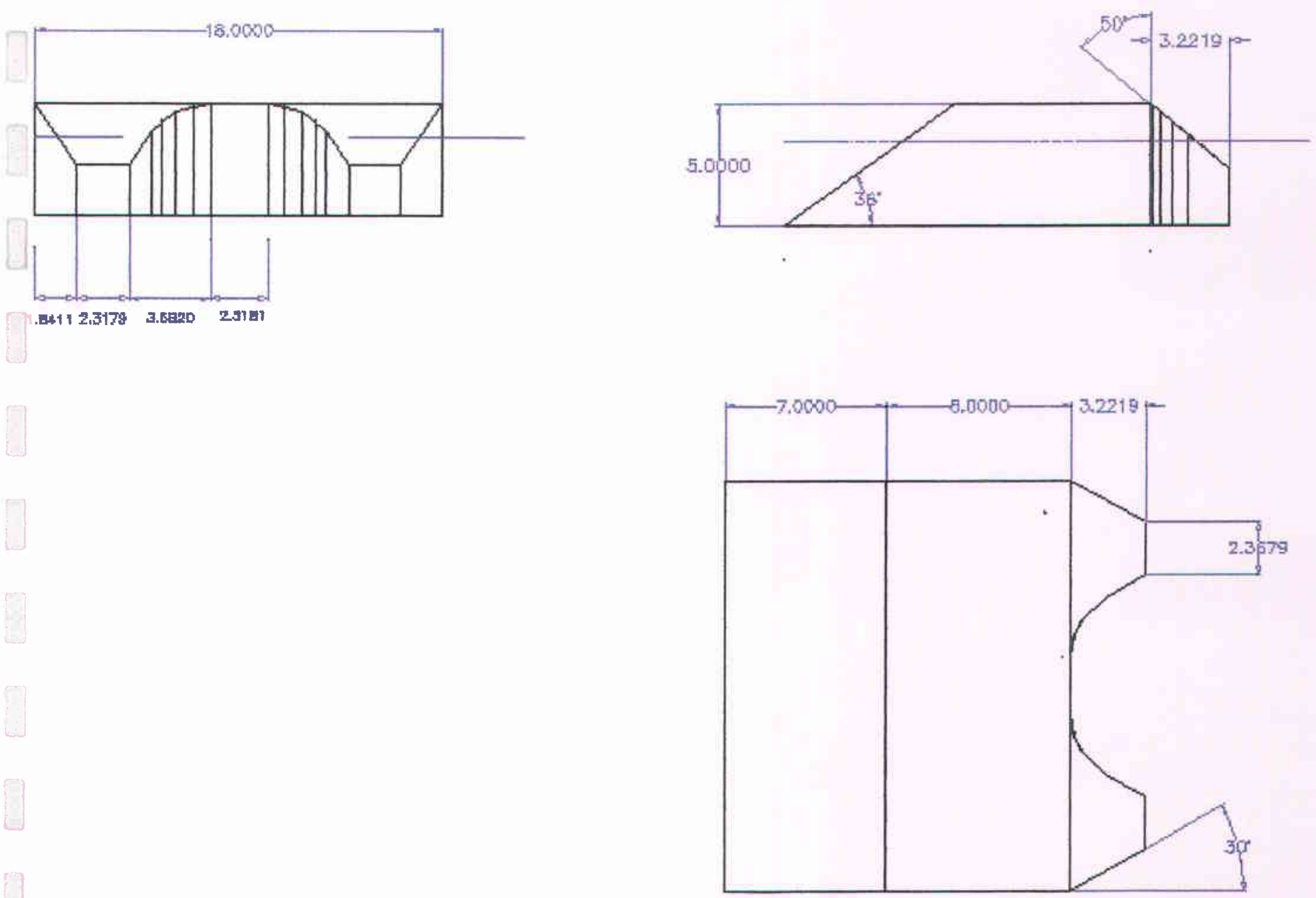

18.0000
2.3179
3.6820
2.3181
5.0000
36°
50°
3.2219
7.0000
6.0000
3.2219
30°

Figure 7

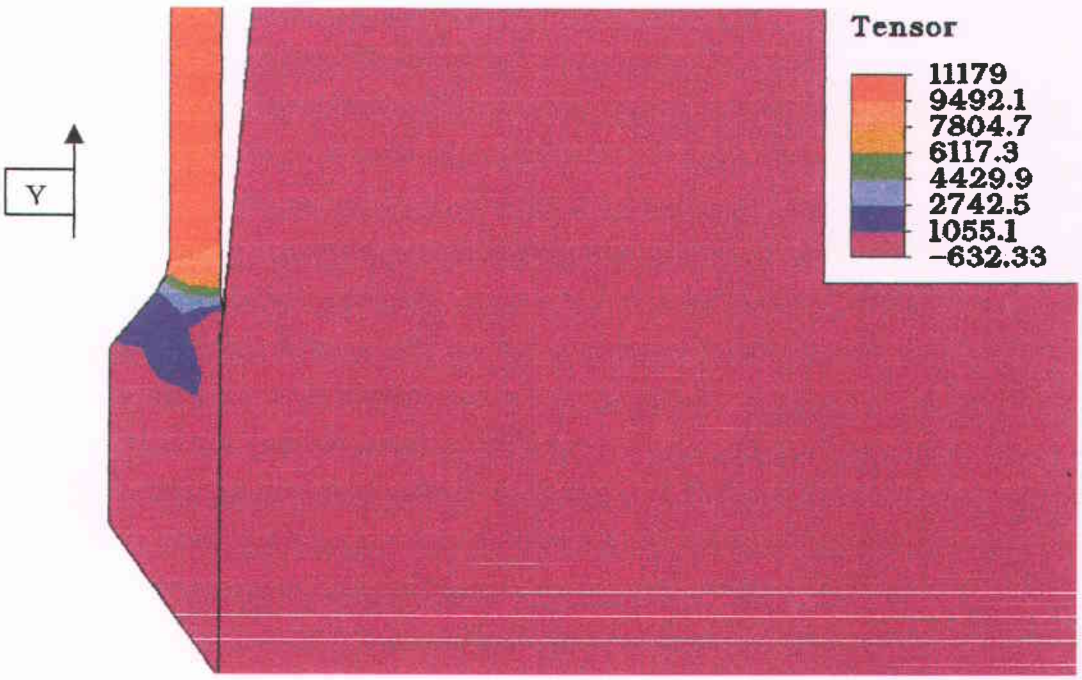

Figure 8

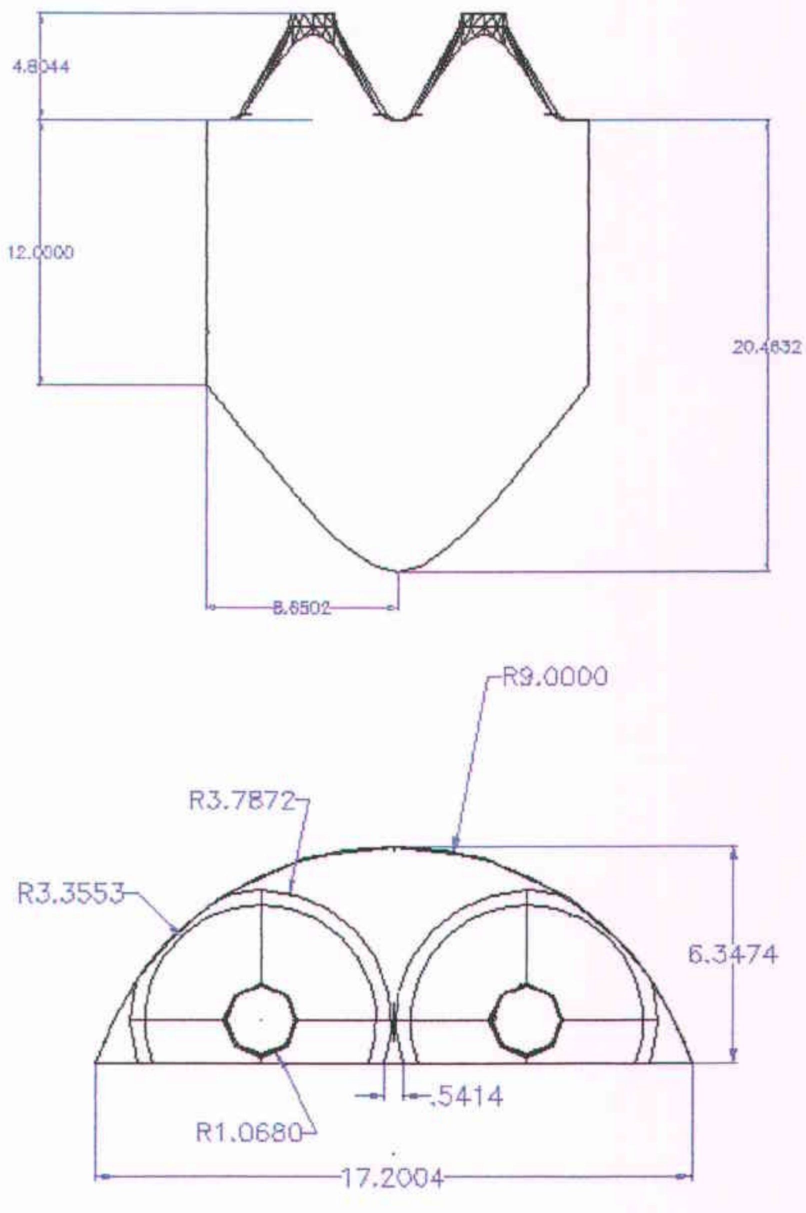
4.8044
12.0000
20.4632
8.6502
R9.0000
R3.7872
R3.3553
6.3474
.5414
R1.0680
17.2004

Picture 1